The hidden biotic face of microbialite morphogenesis – a case study from Laguna de Los Cisnes, southernmost Patagonia (Chile)

Pollier, Clément G. L.; Guerrero, Alejandro N.; Rabassa, Jorge; Ariztegui, Daniel

How to cite

POLLIER, Clément G. L. et al. The hidden biotic face of microbialite morphogenesis – a case study from Laguna de Los Cisnes, southernmost Patagonia (Chile). In: Sedimentology, 2024, p. sed.13189. doi: 10.1111/sed.13189

This publication URL: https://archive-ouverte.unige.ch/unige:175598

Publication DOI: 10.1111/sed.13189

SEDIMENTOLOGY the journal of the International Association of Sedimentologists IAS

Sedimentology (2024) doi: 10.1111/sed.13189

The hidden biotic face of microbialite morphogenesis – a case study from Laguna de Los Cisnes, southernmost Patagonia (Chile)

CLÉMENT G. L. POLLIER*,[1], ALEJANDRO N. GUERRERO†, JORGE RABASSA‡ and DANIEL ARIZTEGUI*

**Department of Earth sciences, Université de Genève, 13 Rue des Maraîchers, Geneva 1205, Switzerland (E-mail: clement.pollier@earth.miami.edu)*

†Centro Universitario Porvenir, Universidad de Magallanes, 739 Manuel Señoret, Porvenir 6300000, Chile

‡CADIC-CONICET, 200 Bernardo Houssay, Ushuaia 9410, Argentina

Associate Editor – Giovanna Della Porta

ABSTRACT

Microbialites provide geological evidence into Earth's early ecosystems, recording long-standing interactions between co-evolving life and the environment. Yet, after more than 100 years of research, the complex interplay between environmental and biological forces involved in microbialite growth is still debated. Laguna de Los Cisnes, located in Chilean Tierra del Fuego, Patagonia, provides a unique opportunity to study these interactions. This lake, which became ice-free around 10 000 years ago, features carbonate microbialites developed by algal–microbial communities. Macroscopically, the organo-sedimentary deposits exhibit a consistent primary crater-like architecture, showcasing macrostructural variations such as dish-shaped, hemispherical, columnar and lenticular morphologies. This study explores the environmental and biological factors shaping microbialite macrostructure by analysing the distribution of dominant morphotypes across the basin. Concurrently, it examines the internal mesostructure and microstructure of microbialites in association with prevailing algal–microbial communities. The incremental development of these communities contributes to the distinct crater-like morphology observed in microbialites from Laguna de Los Cisnes. The mineral encrustation of the green alga *Percursaria percursa* emerges as a primary driver of lithification, evidenced by the preservation of microfossils within the microstructure of the microbialites. Simultaneously, physical environmental factors, including waves, Langmuir cells and accommodation space influence the location of the algal–microbial carbonate factory, determining the spatial distribution and temporal succession of different crater architecture variants. Laguna de Los Cisnes, hosting well-preserved subfossil outcrops and living microbialites, serves as a remarkable living laboratory for understanding microbialite morphogenesis. This study contributes to a novel model that captures the fundamental role of algal–microbial communities in determining the primary macrostructural architecture of microbialites before environmental factors come into play, merely reshaping this architecture into different morphotypes.

[1]Present address: Department of Marine Geosciences, Rosenstiel School of Marine, Atmospheric, and Earth Science, University of Miami, 4600 Rickenbacker Causeway, Miami, FL 33149, USA

Keywords Algal–microbial communities, lacustrine environment, macrostructure, microbialites, Patagonia.

INTRODUCTION

Appearing more than 3.4 Ga, microbialites represent one of the most persistent ecosystems on Earth while being the oldest witnesses of the combined evolution between biosphere, geosphere and atmosphere (Des Marais, 1991; Awramik, 1992; McNamara & Awramik, 1992; Grotzinger & Knoll, 1999; Schopf *et al.*, 2007; Bosak *et al.*, 2013). Throughout this extensive history, microbialites have exhibited a diverse array of structural characteristics across various scales, including macrostructure, mesostructure and microstructure (Grey & Awramik, 2020). These multiscale features provide insights into the interaction between algal–microbial assemblages and the environmental conditions shaping these organo-sedimentary deposits through geological time (Bourillot *et al.*, 2020). Among these features, the macrostructure of microbialites holds particular significance because it is often one of the best-preserved characteristics of microbialites in the geological record, where internal fabric and other algal–microbial microstructures are typically more susceptible to taphonomic processes (Planavsky & Ginsburg, 2009).

The term 'microbialite macrostructure', as outlined by Grey & Awramik (2020), refers to observable characteristics at the naked eye's scale, encompassing the three-dimensional shape of microbialite buildups and their spatial relationships. In the extensive history of microbialite studies, initial investigations considered microbialites as microbial fossils and used macrostructure for taxonomic classification (Krylov, 1976; Semikhatov & Raaben, 2000). Simultaneously, authors attempted to identify evolutionary trends in microbialite macrostructure, aiming to use them as a biostratigraphic tool (Walter, 1972; Bertrand-Sarfati & Walter, 1981). The limitations of this approach led to a shift in perspective, with recent models speculating that physical environmental factors primarily determine microbialite shape (Logan *et al.*, 1974; Gebelein, 1976; Playford, 1980; Trompette, 1982; Grotzinger & Knoll, 1999; Andres & Reid, 2006; Basso *et al.*, 2013). The recent surge in astrobiology has revived debate on the significance of microbialite macro-morphology (Grotzinger & Rothman, 1996; Bosak *et al.*, 2013; Suosaari *et al.*, 2019a). The complexity in defining microbialite macrostructures across the geological record stems from their multifaceted origin, arising from a synergistic interplay of physical, chemical and biological processes (Walter, 1977; Trompette, 1982; Grotzinger & Knoll, 1999). However, the respective contributions of these processes, while recognized, have historically remained ambiguous (Walter, 1977; Semikhatov *et al.*, 1979; Ginsburg, 1991; Suosaari *et al.*, 2019a).

Modern and subfossil microbialites from Laguna de Los Cisnes (Tierra del Fuego, Chile) provide new data to constrain the order of importance of factors in controlling the morphogenesis of microbialites at the macroscopic scale. Microscopic examination of algal–microbial communities colonizing this glacial basin unveils successive morphogenetic stages in microbialite development, leading to the formation of the fundamental crater-like macrostructure observed in most microbialites within Laguna de Los Cisnes. Simultaneously, comprehensive field studies and satellite imagery analysis uncover spatiotemporal variations in the macrostructural characteristics of the individual microbialite craters, including their height, degree and orientation of elongation, and lateral interconnection. Utilizing these morphological criteria, microbialite macrostructure in Laguna de Los Cisnes was classified into five primary morphotypes, whose distribution in the basin correlates with spatiotemporal variations in physical environmental parameters such as accommodation space, wave action and Langmuir cells. Deconstructing the biotic versus abiotic processes shaping the macrostructure of microbialites in Laguna de Los Cisnes contributes to developing a model that advances the understanding of the various individual factors influencing algal microbialite macrostructures over their extensive geological history.

STUDY SITE

Laguna de Los Cisnes (LLC) is located near the north-western coast of the Chilean section of Isla Grande de Tierra del Fuego, 3 km east of the Strait of Magellan (Fig. 1). The region,

Fig. 1. Satellite image showing the geographical situation of Laguna de Los Cisnes (white star) and the series of four other lakes (white dots) located north of the town of Porvenir (red dot).

characterized by low annual average precipitation (283 ± 56 mm) and temperatures (8 ± 3°C), is classified as a Cold Arid Steppe (Peel *et al.*, 2007). Laguna de Los Cisnes is part of a set of lakes, including lagunas La Larga and Verde, as well as lagos Serrano and Deseado located 800 m, 1 km, 6.5 km and 9.5 km further north, respectively (Fig. 1). These topographic depressions located at high latitude (53°14′S, 70°22′W) were formed by the erosive action of the Magellan glacial lobe during the Late Cenozoic Ice Age (Rabassa & Clapperton, 1990; Rabassa *et al.*, 2000; Diáz Balocchi *et al.*, 2021). On the path of this irregular terrain, the complete retreat of the Fuegians glaciers produced the so-called 'Magellan outwash plain' (Coronato *et al.*, 1999; Rabassa *et al.*, 2000) at the end of the Last Glacial Maximum (McCulloch *et al.*, 1997). This geomorphological configuration led to the rapid filling of the LLC basin with a large primitive lacustrine body probably around 10 000 years ago (Auer, 1956; Coronato *et al.*, 1999; Rabassa *et al.*, 2000). The surface of this palaeolake is evidenced by an ancient shoreline located at 13 m above sea level (a.s.l.) in the basin (Figs 2A and S1). Today, the water level is stabilized 6 m lower, creating two hypersaline water masses separated by a land peninsula (Figs 1 and 2A). Despite the proximity of neighbouring lacustrine depressions (Fig. 1), only Laguna de Los Cisnes supports extensive algal–microbial communities and the concurrent development of

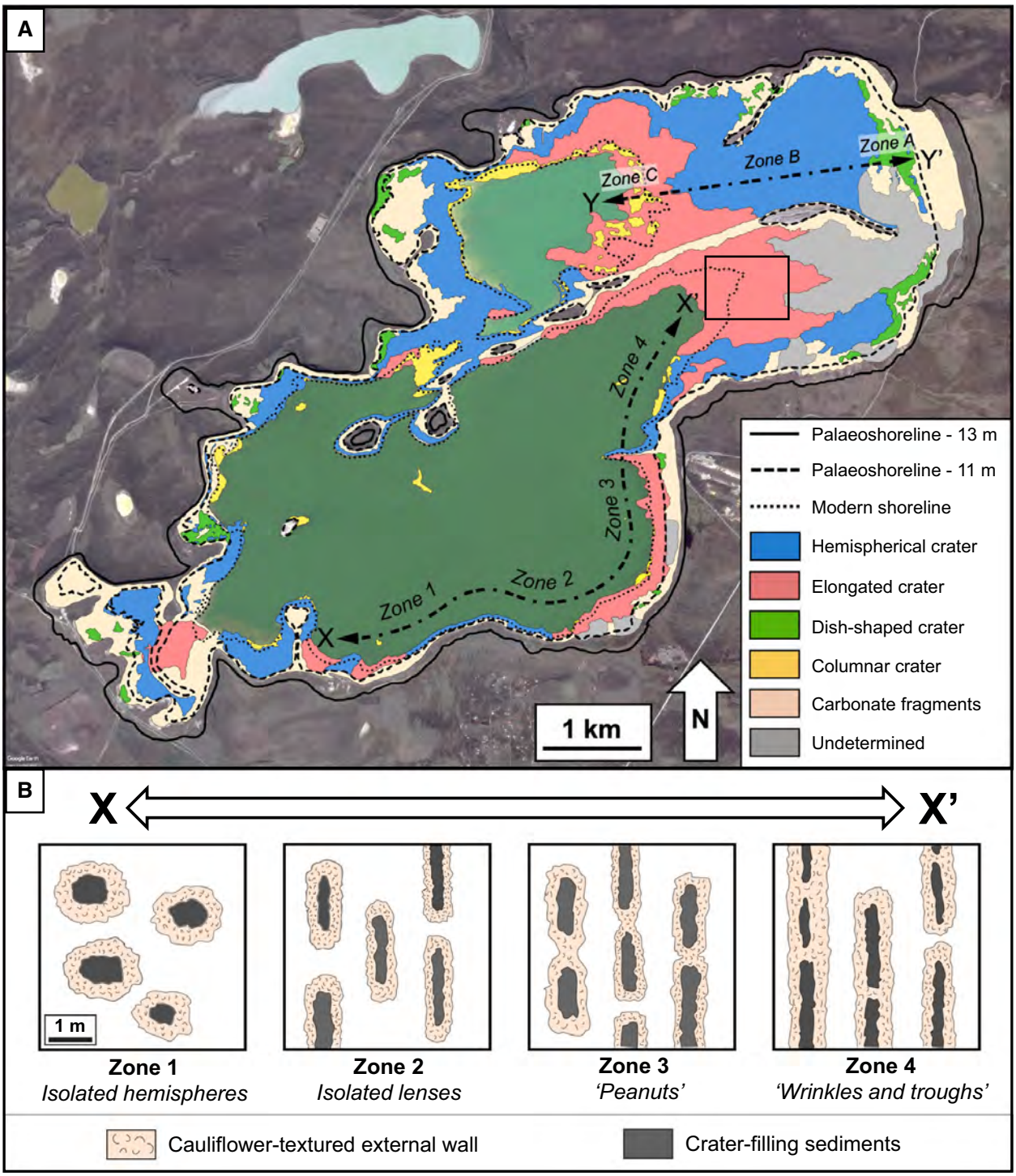

Fig. 2. (A) Map of the distribution of the different microbialite morphotypes colonizing the Laguna de Los Cisnes (LLC) basin as defined in this study. The positions of the ancient and current coastlines are indicated. The arrows emphasize two primary patterns of macrostructural diversity observed in the microbialites of the LLC. These patterns are delineated by specific morphotypes within distinct morphological sub-zones. Sub-zones 1, 2, 3 and 4 correspond to variations in microbialite elongation parallel to the coastline, while sub-zones A, B and C correspond to variations in microbialite height relative to the coastline. The 'carbonate fragments' category corresponds to areas of the LLC basin covered by fragmented microbialites without apparent morphology. Areas covered with vegetation or partially flooded, where it was impossible to map microbialite morphology both in the field and from satellite imagery, are referred to as 'undetermined'. (B) Sketches representing the pattern of lateral morphological variation of microbialites along the X–X' trend shown on the map. The scale is consistent across all drawings.

carbonate microbialites. This specificity is attributed to LLC's unique geochemical characteristics, featuring elevated pH (9.1 ± 0.6) and salinity (52 ± 8‰). Over 900 000 microbialites, occurring either as isolated buildups or coalesced formations, cover both submerged and exposed regions within the basin of Laguna de Los Cisnes, spanning an area of nearly 14 km^2. These organo-sedimentary deposits are currently growing in association with algal–microbial communities in the flooded areas of the LLC, while subfossil microbialites cover the rest of the basin up to 11 m a.s.l., which coincides with an older shoreline (Figs 2A and S1).

MATERIAL AND METHODS

In February 2020, a multidisciplinary team of Swiss, Chilean and Argentinian researchers conducted a detailed field investigation at Laguna de Los Cisnes to pinpoint key environmental and biological factors influencing the macrostructure and distribution of carbonate buildups across the basin.

Analysis of environmental parameters

Lake level variations since 1986 were reconstructed using the 'timelapse' function of Google Earth Pro software (Version 7.3.3). A high-resolution (4800 × 3689) image of the LLC obtained from this same software formed the basis for identifying the different coastlines that characterize the geomorphology of the basin. These data were correlated with historical lake descriptions (Jory *et al.*, 1974; Cordero, 2007; Fuentes & Gajardo, 2017) and plotted using Adobe Illustrator (Version 24.3). To ascertain the elevation of successive coastlines relative to the height of algal–microbial buildups, topographic profiles along the basin flanks were acquired using Global Mapper software (Version 22.1; Blue Marble Geographics, USA) and relied on the ALOS World 3D – 30 m (AW3D30) global digital surface model. This approach provided a more precise understanding of the lateral and vertical extent of temporal changes in the LLC level and their impact on the microbialite system in the basin.

Meteorological data come from the meteorological station N°530 005 at Capitán Fuentes Martínez airport, located 200 m east of the lake. Records of rainfall, wind and temperature since 1985 were obtained from the Dirección Meteorológica de Chile website (https://climatologia.meteochile.gob.cl). All statistical analyses (average wind speed and direction, persistence of winds) from the raw data were performed using Excel software. The monthly average measurements of wind speeds and directions were plotted with WindRose Excel (Version 1.7).

Analysis of algal–microbial communities and microbialite microstructure

Salinity and pH measurements were conducted on-site using a Multi 3400i Handheld Multimeter (WTW, Weilheim, Germany). Fresh segments of algal–microbial mats were preserved in plastic containers, maintaining submersion in the lake water. Upon returning to the laboratory, multiple subsamples of these communities were promptly fixed in plastic vials filled with lake water containing 1.0% (v/v) glutaraldehyde and stored at 4°C. Smear slides were prepared by gently pressing a piece of biofilm, previously rinsed with distilled water, between a glass slide and a cover slip. Concurrently, thin sections of microbialite samples were crafted at the Thin Section Laboratory at the University of Geneva (Switzerland). All samples were examined through an Olympus BX61 (Olympus, Tokyo, Japan) optical microscope.

Morphometric analysis of microbialites

The macroscopic characteristics of the microbialites in Laguna de Los Cisnes were mapped across the basin by integrating geological field data (observations, sampling, GPS measurements). The macrostructural description of microbialites is based on the conceptual framework proposed by Kennard & Burne (1989) and Grey & Awramik (2020), and relies on various macroscopic features, including 3D shape, dimensions, linkage and degree of preservation of microbialites. Geometric analysis enabled the categorization of microbialites into morphological types, referred to as 'morphotypes', based on the height-to-width ratio (H/W) of individual structures in vertical view. A H/W ratio >1.2 designates a column, while a H/W ratio <0.8 indicates a dish-shaped microbialite. Hemispherical and lenticular shapes, sharing H/W ratios between 0.8 and 1.2, are differentiated based on their degree of elongation in plan view. The length-to-width ratio (L/W) determines this elongation, with structures having an L/W ratio above three classified as lenses (lanceolate to

ovate plan view), and those below three defined as mounds (circular plan view). For elongated microbialites, the orientation of the elongation axis with respect to the north was measured in the field using a compass. By employing this classification system and directly measuring microbialite dimensions and orientations in the field, the distribution of these morphotypes in the basin was mapped using Adobe Illustrator (Version 24.3).

This dataset has been integrated with satellite images, allowing the direct measurement of both the horizontal dimensions and orientation of microbialites. The images used for analysis had a resolution suitable for the metric dimensions of algal–microbial deposits and were obtained through Google Earth pro 7.3.2 (CNES/Airbus images: Natural colours), Sentinel Hub (Sentinel-2 L2A images: Natural colours [4,3,2], Infrared [8,4,3], NDWI [8 − 4/8 + 4]; Landsat 8: Natural colour and False colour) and USGS Earth Explorer. Excluding images with excessive cloud cover or water turbidity, the selected satellite images for mapping were obtained in summer when the lake level was minimal, revealing a greaterhy: A derivative of the Encyclopedia of Ocean Sci extent of emerged microbialites in the basin. To accentuate the relief associated with the structures, all images were examined in false colour.

RESULTS

Lake level variations

The highest palaeoshoreline affecting the LLC basin is located at 13 m a.s.l. (Figs 2A and S1). Beneath this initial ancient shoreline, a steppe extends to 11 m a.s.l., where a second palaeoshoreline imprints the lake margins (Figs 2A and S1). This second, comparatively lower palaeolake highstand coincides with the sudden appearance of microbialites. Those emerged algal–microbial constructions are associated with broad bands of dry beaches surrounding the present lake surface at 7 m a.s.l. (February 2020; Figs 1, 2A and S1). This modern shoreline correlates with a shift in microbialite colouration (Figs 7B, 7C and 9B). Submerged microbialites are red, indicative of freshly precipitated limestones associated with decomposing algal–microbial mats on the surface of deposits. In

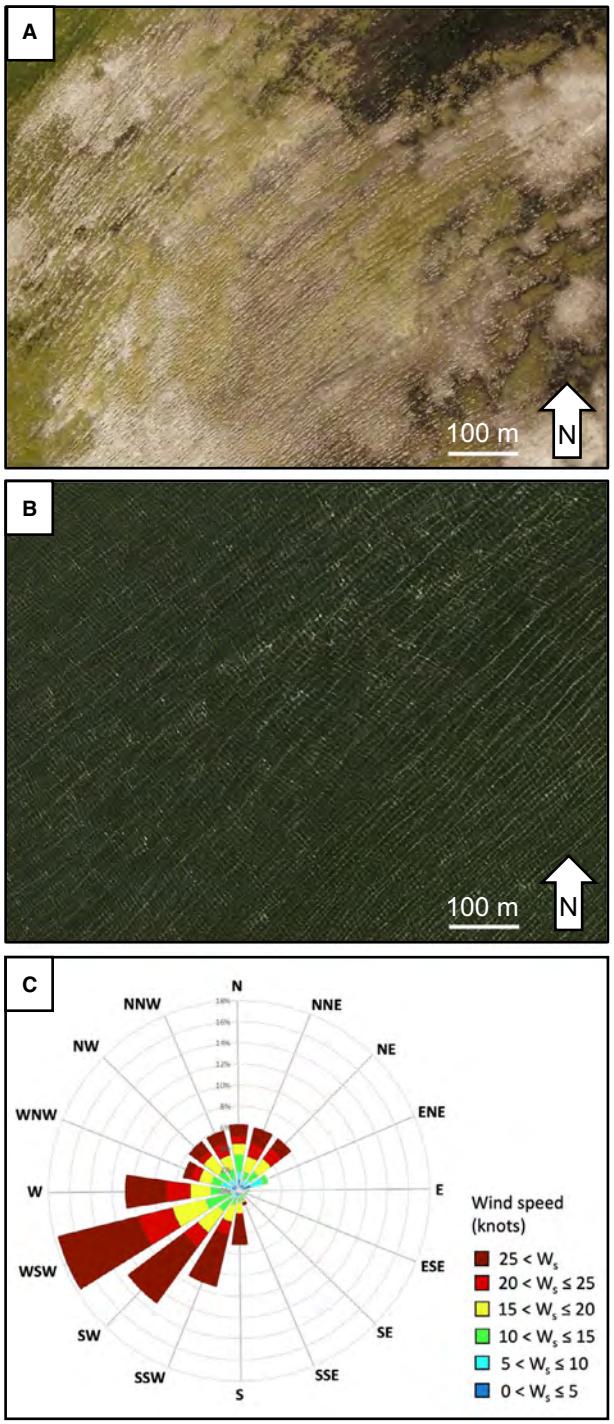

Fig. 3. (A) Alignments of elongated 'wrinkles and troughs' type microbialites on the eastern shore of the lake (box area in Fig. 2). (B) 'Windrows' created by Langmuir circulations at the surface of the north-eastern part of the lake. (C) Wind strength and orientation during February 2020 measured from the meteorological station at the Capitan Fuentes Martinez Airport, located 200 m east of Laguna de Los Cisnes.

contrast, emerged microbialites showcase a beige hue, typical of older limestones that have been exposed and undergone partial dissolution. This colour gradient marks the distinction between fossilized carbonates whose construction has ceased and 'active' microbialites associated with living algal–microbial mats.

Dominant hydrodynamic forces

The region is influenced by persistent westerlies, generating Langmuir circulations (LCs) in the basin, which consist of shallow counter-rotating vortices oriented in line with the wind direction (Fig. 10). These give rise to regularly spaced and parallel windrows at the lake surface that align with a persistent south-west/north-east orientation (Fig. 3B and C). Long-term satellite observations confirm that this circulation pattern is maintained for extended periods of time due to the persistence of regional winds. The hourly measurement of February 2020 (Fig. 3C) indicated that the winds: (i) came for 60.8% of the cases from the south-west quarter; and (ii) were above six knots (the minimum speed required for the creation of Langmuir cells in the water column; Langmuir, 1938; Smith, 2001; Leibovich, 2009) during 91.4% of the time (23.7 ± 13.5 knots in average). Despite the limited fetch length of the system, the shores of the LLC experience persistent wind-induced large waves, occasionally surpassing 1 m in height, with heightened intensity along the windward margin on the east side of the basin.

The biological component – algal–microbial communities and microbialite microstructure

The submerged shorelines of the LLC basin host extensive algal–microbial communities, uniformly dominated by the filamentous green algae *Percursaria percursa* (refer to Appendix S1 and Fig. S2 for a detailed description). To a lesser extent, these algal–microbial assemblages also exhibit a diverse array of diatoms, cyanobacteria and other green algae species, coexisting within a dense Extracellular Polymeric Substances (EPS) layer about 1 cm thick. These communities form benthic mats that cover extensive areas of Laguna de Los Cisnes, including the deepest sections of the lake (Fig. 4A). Near coastal and shallower areas, filamentous networks from these benthic mats tend to reach towards the lake surface, buoyed by gas bubbles trapped within the EPS (Figs 4A and 5D). Consequently, patches of algal–microbial communities emerge at the water surface (Figs 4B, 4C and 5B), laterally linked to the benthic layer of the mat. The floating section of the mat is closely associated with growing microbialites, and frequently covers flooded organo-sedimentary structures with an organic sheet several millimetres thick (Fig. 4B, C and D). When emerged during annual lake level fluctuations, these biofilms rapidly dry out, forming a rigid white envelope encrusted by calcium carbonates that surrounds the microbialites (Fig. 4B and D). Smear slides of the partially desiccated biofilm showcase abundant *Percursaria percursa* filaments coated with calcium carbonate (Fig. S2).

The indurated surface of LLC microbialites features cauliflower-like structures (Fig. 5C) reminiscent of the swellings created by gas bubbles entrapped at the surface of the algal–microbial biofilm (Fig. 5D). Detailed examination of the microbialite surface reveals a granular appearance composed of cemented spheres roughly 1 mm across (Fig. 5E). *Artemia persimilis* eggs adhered within the *Percursaria percursa* biofilm match the size and shape of these granules (Fig. 5F). Beneath the hardened surface, the mesostructure of the microbialites is layered, with carbonate deposits parallel to the surface and interspersed with remnants of desiccated white biofilms (Fig. 5A). These layers, primarily composed of monohydrocalcite (see Appendix S2 and Fig. S3 for more information), exhibit indentations reminiscent of folds observed in living algal–microbial biofilms (Fig. 5A and B). Microscopically, these layers contain tubular microfossils resembling *Percursaria percursa* filaments (Figs 6 and S2), with a central cavity encased in concentric mineral layers. Around those microfossils, the interstitial space is partially filled with clotted peloidal micrite that occasionally transitions laterally into microsparite (Fig. 6). This microbialite internal structure is similar across bioherms collected from different locations and depths within the basin.

The microbialites – morphological types

The microbialites of the LLC exhibit significant morphological diversity, yet a dominant architecture common to all deposits can be distinguished. This shared framework displays a 'crater' shape characterized by a carbonate wall encircling an interior space, partially filled with sediments and water in the flooded microbialites (Figs 7A, 7B, 7D and 8B). Frequently, the flanks

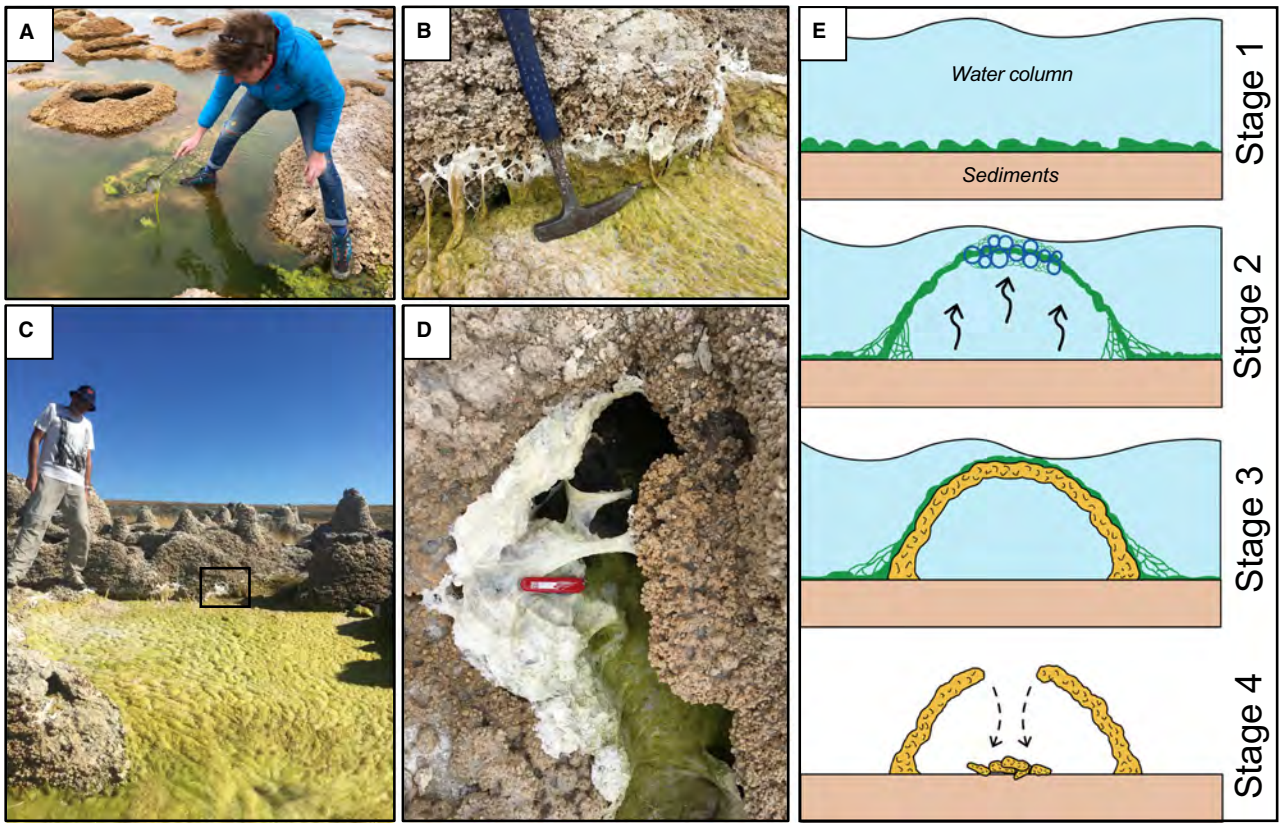

Fig. 4. (A) Benthic algal–microbial mats developing at the bottom of the lake and rising towards the surface as a result of most probably oxygen bubbles trapped in the filamentous matrix. The person's shoes are 27 cm long. (B) Green floating biofilm sticking to the inner wall of a cratered microbialite. The emerged parts are completely dry, forming a rigid and white layer on the surface of the microbialite (box area in Fig. 4C); scale (length of hammer head) = 18 cm. (C) Biofilm floating at the surface of the inner pool of a microbialite crater. The height of the person is 175 cm. (D) A completely dry biofilm forming a rigid layer covering the inner surface of a cratered microbialite. Note the elasticity of these biofilms that connect two microbialites by a rigid 'bridge' made of dried filamentous green algae; scale (knife width) = 1.5 cm. (E) Sketches showing the proposed stages of formation and evolution of the microbialite crater shape (refer to text for explanation).

of the crater converge upward towards the centre of the structure, leading to its complete closure. In this case, the microbialites form a completely hollow dome (Figs 7D and 8A). From this fundamental crater architecture, microbialite macrostructure differentiates into four main morphological variants with specific distribution within the LLC basin: mounds, columns, lenses and dish-shaped microbialites (Figs 7 and 8). Microbialite crusts represent a fifth morphotype occurring the Laguna de Los Cisnes, the only one without a crater-like organization (Fig. 8D).

Mounds morphotype

The mounds are the typical crater-like microbialites encountered in the LLC, characterized by a half-spherical shape of variable dimensions: 0.15 cm to 2.50 m in diameter for an equivalent height (Fig. 7A). This morphotype is the most frequent, generally encountered at intermediate altitude (7–10 m a.s.l.) on the western coast of the basin, where it covers vast areas by a continuous encrustation of unlinked buildups (Fig. 2A).

Dish-shaped morphotype

This morphotype is dominated by lateral growth, producing a carbonate wall delimiting an extended internal basin whose irregular surface sometimes exceeds 18 m^2 (Fig. 7B). Conversely, the relief of the dish-shaped microbialites is limited, rarely exceeding 30 cm. As the growth of these deposits is essentially

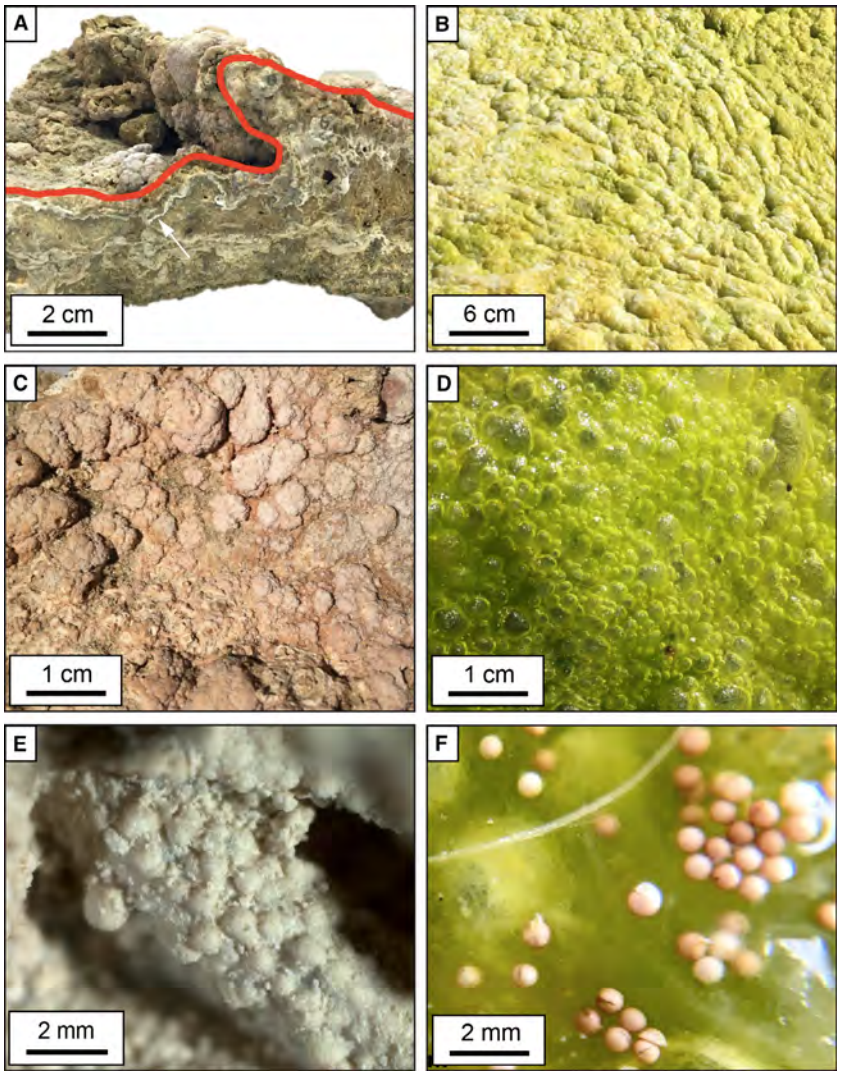

Fig. 5. Contrasting textures observed on the surface and within microbialites (left panel) with those present in living algal–microbial communities from Laguna de Los Cisnes (right panel). (A) Cross-sectional view along the roof of a dome-shaped microbialite in Laguna de Los Cisnes unveils a stacking of folded carbonate layers aligned parallel to the surface of the structure. Note the presence of a residue of white desiccated and encrusted algal–microbial mat just below the surface (white arrow). (B) Surface of the floating section of a living algal–microbial community displaying a similarly folded texture caused by wave action. (C) Cauliflower-like structures covering the indurated surface of microbialites. (D) Surface textures of the floating section of algal–microbial biofilms, interspersed with swellings formed by entrapped gas bubbles. (E) Close-up view of the surface of microbialites from Laguna de Los Cisnes, revealing the ubiquitous presence of small, cemented spheres contributing to the granular appearance. (F) *Artemia persimilis* shrimp eggs trapped between filaments of *Percursaria percursa* and the sticky extracellular polymeric substances of the algal–microbial communities.

horizontal, the buildups are systematically coalescent and form thick and continuous biostromes that uniformly cover the higher areas of the basin (10–11 m a.s.l.; Fig. 2A).

Column morphotype

The pinnacle morphotype includes the tallest microbialites found in the lake, reaching as high as 5 m, with a perfectly cylindrical profile (Fig. 7C). They are systematically organized as isolated colonies, made up of a dense aggregation of dozens of individuals (Fig. 7C). Bioherms made of coalescent columnar structures generally develop far from the coast, in the deepest areas of the lake (5–7 m a.s.l.; Fig. 2A). Their distribution is very discontinuous, each columnar cluster being separated by several hundred metres.

Lenses morphotype

This variant of the crater architecture is characterized by a central cavity elongated along an axis of variable orientation (Fig. 8A, B and C). This morphotype displays the same altitudinal distribution as the mounds but dominates the eastern – windward – shores of the lake (Fig. 2A). The degree of elongation is highly variable from one structure to another, with a length-to-width ratio varying from 3 to 15 (Figs 2B, 8A, 8B and 8C).

Crusts morphotype

Contrary to other crater-shaped microbialites, this morphotype occurs as a thin carbonate crust enveloping a nucleus of variable dimensions, ranging from small pebbles to metric blocks (Fig. 8D). Note that the encrustation is non-uniform and tends to develop preferentially on the top of

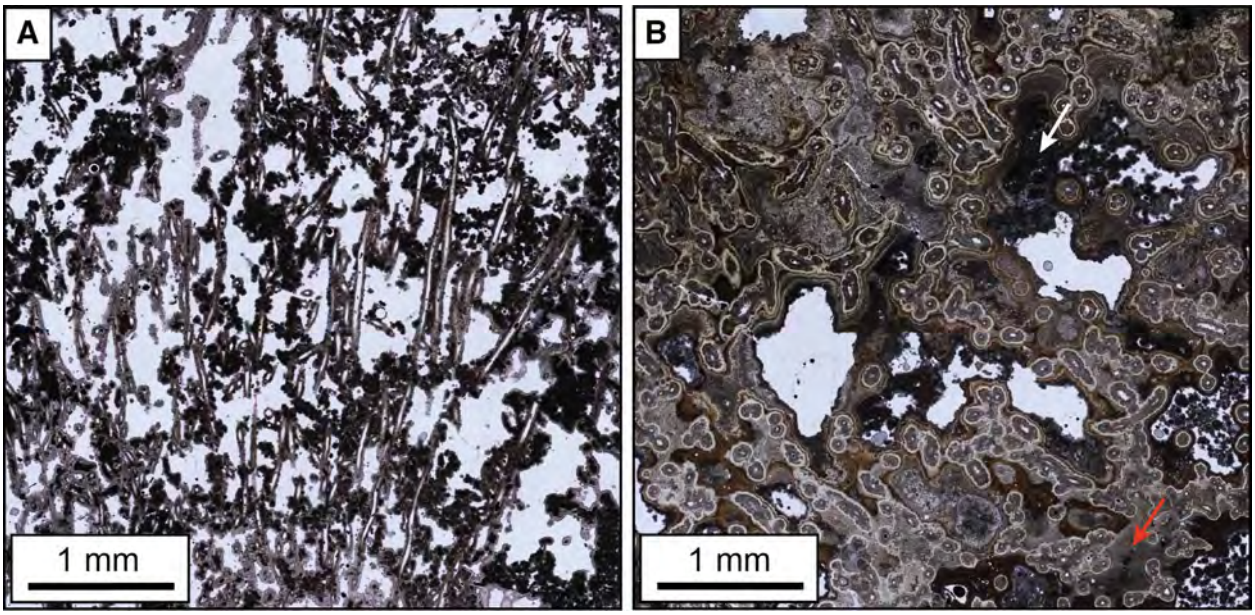

Fig. 6. Microscopic network of mineralized filamentous features comprising the internal structure of microbialites in Laguna de Los Cisnes, as seen in a longitudinal section (A) and perpendicular section (B) to the lateral wall of these microbialites. These filamentous structures feature a circular and elongated central cavity surrounded by concentric mineral layers, mirroring the dimensions and morphology of the mineral encrustation surrounding *Percursaria percursa* filaments encountered in living algal–microbial communities of Laguna de Los Cisnes. These tubular microfossils are surrounded by a microsparite, which is generally structureless (red arrow), but occasionally exhibits fine laminations. This microsparite laterally transitions into clotted peloidal micrite (white arrow).

the nucleus, exhibiting the same surface texture as the crater-shaped microbialites (Fig. 8D). Due to the low availability of potential encrusting substrates on the lake floor, this morphotype is rarely encountered in the LLC. Active forms only occur occasionally in the deepest parts of the basin (<5 m a.s.l.).

Distribution of morphotypes

The distribution of the previously defined morphotypes was further mapped, highlighting the spatial heterogeneity of microbialite shapes at the basin scale (Fig. 2A). Several 'morphotype zones' – i.e. areas of the basin dominated by a specific morphotype (representing at least 80% of the morphotypes included in the area) – have been identified. The distribution of morphotypes in the basin is not arbitrary but rather organized around three specific patterns: (i) a lateral morphological trend parallel to the coastline (X–X' on Fig. 2A); (ii) a lateral morphological trend perpendicular to the coastline (Y–Y′ on Fig. 2A); and (iii) a vertical morphological trend.

Microbialite elongation gradient parallel to the coastline

Along the lake's coastline, a clear morphological transition occurs with microbialites progressively elongating eastward (Fig. 2A and B). This elongation gradient delineates four morphological sub-zones based on two criteria: (i) the length-to-width ratio; and (ii) the orientation of elongated structures. Sub-zone 1 features isolated mounds with a circular plan view, exhibiting no preferential lateral growth (Figs 2B, 7A and 7D). As the buildups extend eastward, they adopt a lenticular morphology typical of sub-zone 2 (Figs 2B and 8A). Further elongation in the same direction leads to two or three neighbouring lenses joining at their extremities, generating a morphological variant with a 'peanut' shape typical of sub-zone 3 (Figs 2B and 8B). In the easternmost regions of the basin, elongation and linkage dynamics in microbialites intensify, and the original lenses are no longer distinguishable, forming a regular alignment of linear bioherms composed of several coalesced microbialites ('wrinkles and

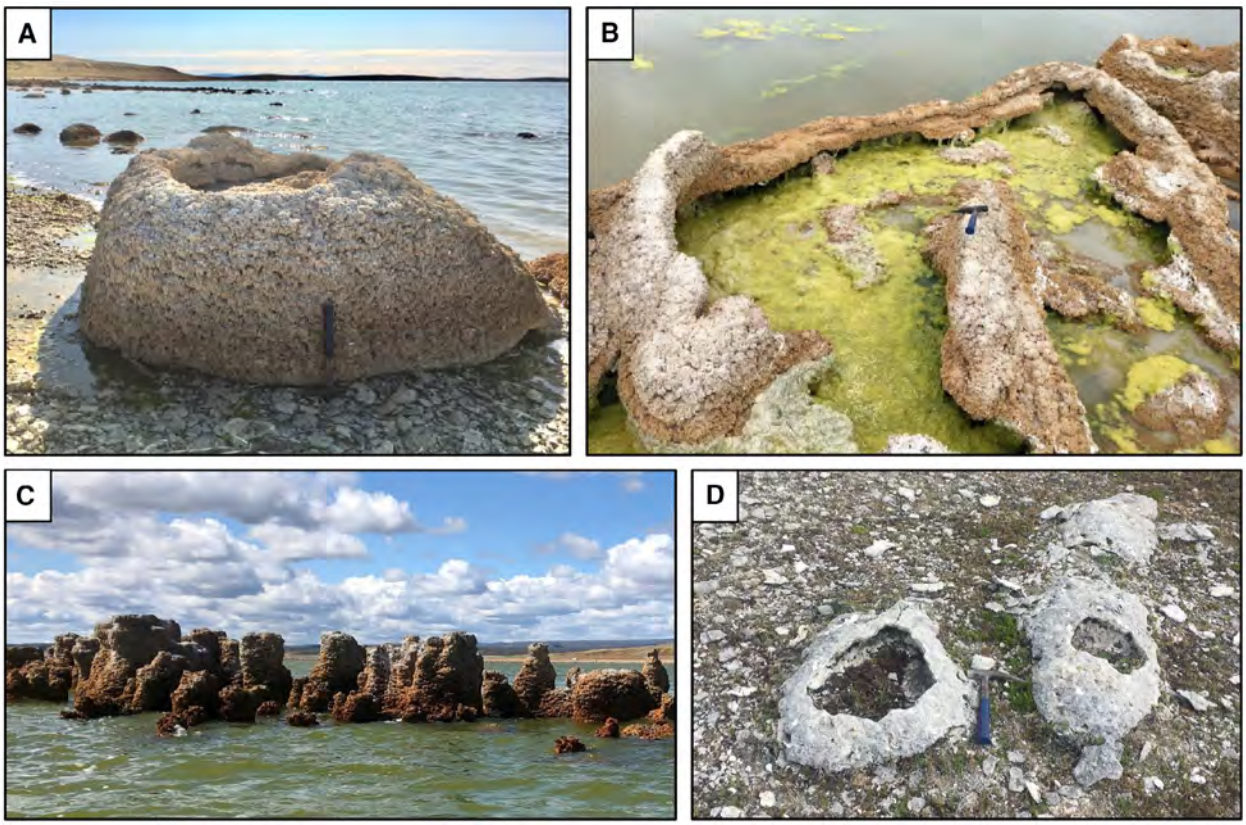

Fig. 7. (A) Subfossil microbialite with a mound morphology; scale (length of hammer) = 32 cm. (B) Dish-shaped microbialite containing living floating algal–microbial communities. The white layer at the top of the structure corresponds to salt deposits resulting from the evaporation of lake water splashed onto the microbialites by the waves; scale (length of hammer head) = 18 cm. (C) Columnar microbialites partially emerging in today's central area of the lake. The height of the columnar microbialites in the centre is 120 cm. (D) Fossilized microbialites of dome shapes in the emerged areas of the basin. Note the collapse of the roof of the structure in the central part of the two in the front resulting in a crater morphology, whereas the smaller one in the back appears complete; scale (length of hammer head) = 18 cm.

troughs'). These structures extend several tens of metres and dominate sub-zone 4 (Figs 2B, 3A and 8C).

Additionally, the orientation of microbialite stretching varies across the lake. In the western regions, the alignment of elongated buildups is controlled by the orientation of the coastline and develops systematically perpendicular to it. Conversely, in the eastern part of the basin, stretching axis orientation is independent of the orientation of the coastline and rather develops a persistent south-west/north-east trend (Figs 2 and 3A). In those windward regions, the orientation and wavelength of the microbialite ridges display a surprising similarity with the characteristics of the LC-induced windrows at the lake surface (Fig. 3A and B), both parallel to the dominant wind direction (Fig. 3C).

Microbialite height zonation perpendicular to the coastline

Another pattern of morphological variation in the LLC microbialites emerges along a transect perpendicular to the coastline. This morphological gradient is characterized by the increasing height of the structure combined with a concomitant reduction of their width towards the centre of the basin. Based on the height-to-width ratio of the microbialites, three morphological sub-zones can be distinguished (Figs 2A and 9A). From the highest to the lowest regions of the basin, there is; sub-zone A (10–11 m a.s.l.) dominated by dish-shaped microbialites, sub-zone B (7–10 m a.s.l.) which encompasses mounds (or more or less elongated lenses depending on the lateral position in the basin; refer to previous section), and sub-zone C (5–7 m a.s.l.) characterized by

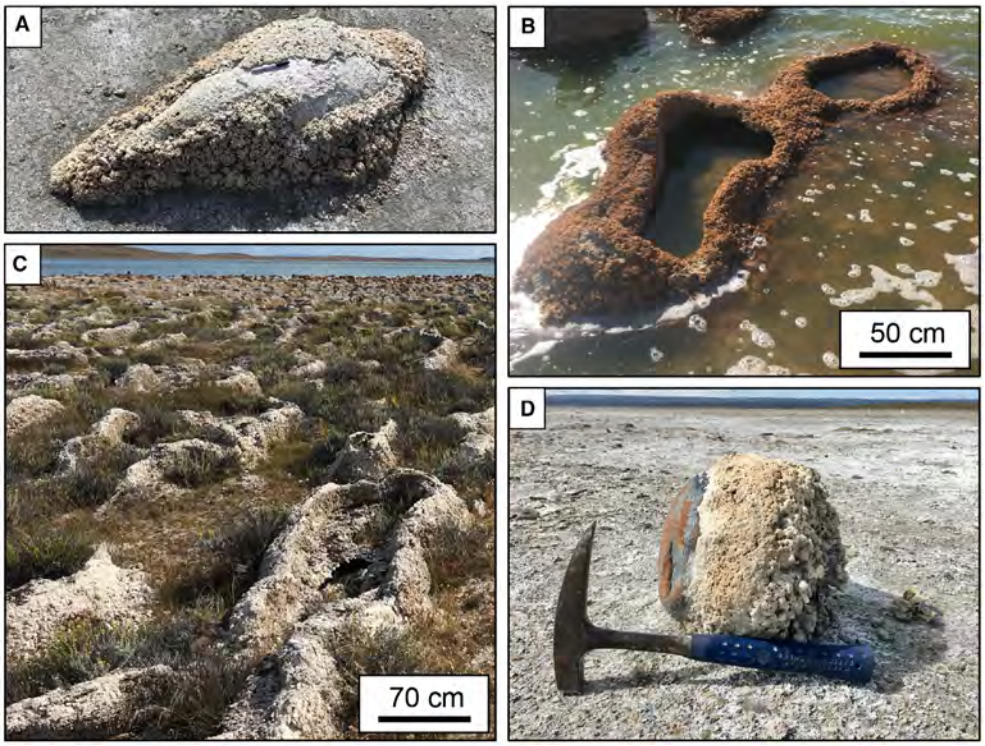

Fig. 8. (A) Elongated lens-shaped subfossil microbialite; scale (length of pen) = 14 cm. (B) Modern elongated 'peanut-shaped' microbialite. (C) North-east coast of the lake showing the uniform alignment of elongated subfossil microbialites with a 'wrinkles and troughs' pattern. (D) Microbialite crust developing on the surface of an isolated pebble in the dry central region of the northern section of the lake. The top of the structure is oriented towards the right side of the image; scale (length of hammer head) = 18 cm.

columnar forms (Fig. 9A). The altitude of the top of most buildups remains constant at 11 m a.s.l., regardless of microbialite morphology or position along the coastal transect (Fig. 9A). An exception to this morphological gradient is the encrusting morphotype in the deepest region of the basin (<5 m a.s.l.), exhibiting limited vertical growth at the top of a nucleus (Fig. 9A).

Vertical morphotype variations and compound microbialites

The individual structures cited so far correspond to a single morphological class clearly identifiable in the field. However, it is common to find so-called 'compound microbialites' on the coasts of the LLC, combining different types of macrostructures alternating during their growth (Fig. 9B). A vertical morphological transition occurs in these bioherms, with the most frequent pattern corresponding to the superposition of a columnar microbialite, culminating at 11 m a.s.l., above a basal mound or lens morphotype whose summit is located at 10 m a.s.l. (Fig. 9B).

DISCUSSION

Microbialite elongation and hydrodynamic conditions in the basin

Elongated microbialites, common in both ancient and modern carbonate settings (Serebryakov & Semikhatov, 1974; Young & Jefferson, 1975; Young & Long, 1976; Button & Vos, 1977; Playford, 1980; Andres & Reid, 2006; Coulson, 2016), have generated numerous theories regarding their development, such as light angle, substrate inheritance, hydrodynamics, etc. (Playford, 1980; Feldmann & McKenzie, 1998; Ginsburg & Planavsky, 2008). The exact role of these processes in ruling – stretching – microbial macrostructures remains unclear (Bosak *et al.*, 2013), but new models are emerging (Mariotti *et al.*, 2014; Coulson, 2016). In Laguna de Los Cisnes, the elongation of microbialites strongly correlates with coastal exposure to westerly winds, implying that hydrodynamic processes induced by the winds are responsible for this morphological

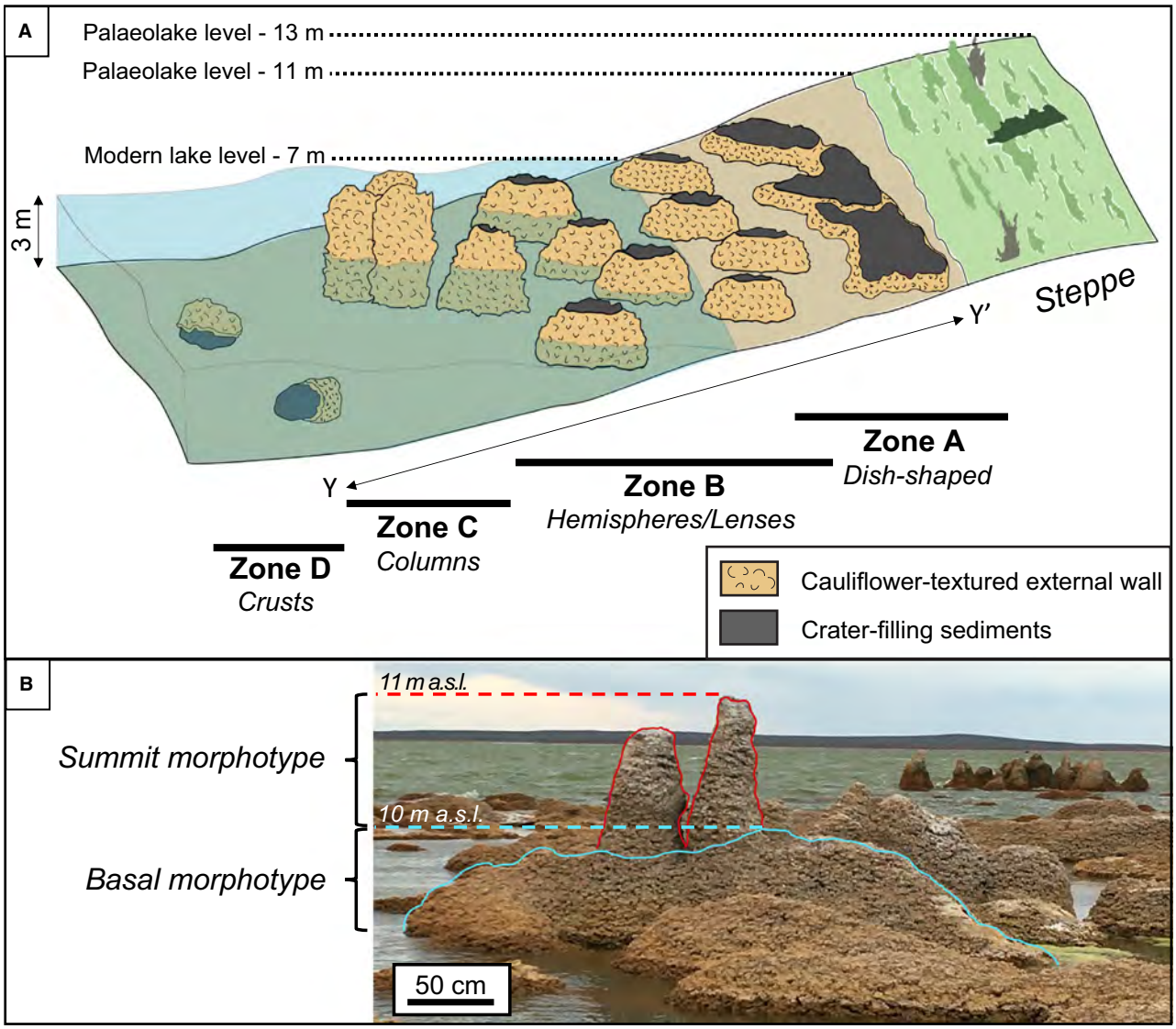

Fig. 9. (A) Sketches illustrating the lateral morphological transition of microbialites, perpendicular to the coastline of Laguna de Los Cisnes (Y–Y′ axis represented in Fig. 2A), in relation to the modern and ancient shorelines. (B) Microbialite with 'compound' morphology, consisting of a columnar morphotype superimposing a lenticular morphotype.

character. This is further developed in the following subsections.

Morphogenic impact of Langmuir cells

In the north-eastern part of the basin, microbialites align with the prevailing winds, developing morphological characteristics similar to those of Langmuir cells (LCs) affecting the LLC water column (Fig. 3). Previous investigations have suggested that such circulation patterns profoundly impact sedimentation both underwater and in the subaerial domain, resulting in the formation of longitudinal sedimentary features (Bagnold, 1953; Dzulynski & Walton, 1965; Allen, 1969; Glennie, 1970; Wilson, 1972). The 'seif stromatolites' in Hamelin Pool (Australia) are good modern analogues, also related to LCs (Playford, 1980; Playford *et al.*, 2013). Those mixing cells are cylindrical so that their depth of influence is equivalent to their width, i.e. half the distance between two successive windrows (Thorpe, 2004; Leibovich, 2009). Therefore, the helicoidal circulation scheme occurring in Laguna de Los Cisnes likely affects not only the

entire water column but also the floor, a common phenomenon in shallow lakes (Dethleff & Kempema, 2007; Leibovich, 2009). Furthermore, the currents they generate transport various elements, including sediments and algal–microbial biofilms (Langmuir, 1938; Gargett *et al.*, 2004; Dethleff & Kempema, 2007; Dierssen *et al.*, 2009; Chubarenko *et al.*, 2018). These data enable the formulation of a model that associates elongated microbialites with LCs (Fig. 10). When these cells are established in the LLC, downwelling currents likely erode the lake substrate at convergence zones, forming troughs, while sediments accumulate at the meeting point of adjacent vortices (Fig. 10). The distribution of algal–microbial mats would also be influenced by this circulation pattern, preferentially colonizing the divergence zones where they consolidate the previously deposited sediments. Over an extended period, the resulting spatial partitioning of sediment depocentre and algal–microbial carbonate factory on the lake substrate would provide an initial pattern for the establishment of elongated microbialites oriented along the LCs axis and parallel to the wind (Fig. 10).

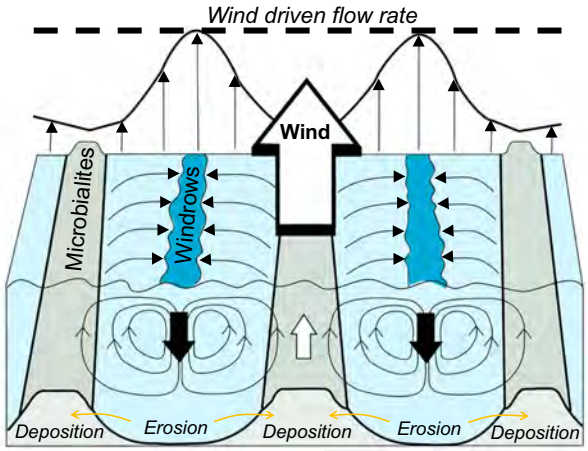

Fig. 10. Diagram illustrating the model of formation of elongated microbialites under the effect of Langmuir circulations affecting the water column of Laguna de Los Cisnes.

Morphogenic impact of waves

Moving towards the less windy western coasts of the basin, elongated microbialites demonstrate a stronger connection to the orientation of the coastline, aligning systematically perpendicular to it. This relationship results in some microbialites orienting at right angles to the prevailing winds in the lake's western region. While Langmuir cells can deviate up to 20 degrees from prevailing winds (Talley *et al.*, 2011), the extreme angles observed in the elongated microbialites contradict the previous model and imply the involvement of another mechanism.

The morphogenetic relationship between elongated microbialites and the coastline is likely influenced by wave action, where wave translation tends to be perpendicular to the coastline in areas with low wind exposure. Such a relationship is common in the geological record, where elongated microbialites often show a preferential orientation that coincides with that of current-related sedimentary structures (Hoffman, 1967; Serebryakov & Semikhatov, 1974; Young, 1974; Young & Jefferson, 1975; Young & Long, 1976; Button & Vos, 1977; Bertrand-Sarfati & Awramik, 1992). In modern systems, Playford (1980) and Andres & Reid (2006) have also demonstrated the importance of moving sediment-laden water in originating this pattern, acting as an abrasive agent that sculpts pre-existing microbialites in the direction of the current.

Yet, the absence of internal sedimentary discontinuities within the LLC microbialites suggests that potential wave action on the elongation process occurs contemporaneously with the growth of the structure by influencing the algal–microbial carbonate factory. Waves concentrate in depressions between coastal microbialites, inhibiting mat growth. Conversely, calmer environments develop on the 'back-side' of the buildups where sediments accumulate, later colonized by thick algal–microbial mats. By influencing the distribution of the organo-sedimentary consortium on the lake substrate, waves accentuate microbialite elongation along prevailing currents roughly perpendicular to the shoreline. In the north-east regions of the basin, waves are also likely to contribute to microbialite elongation, but the strong wind maintains Langmuir cells as the primary influencers of microbialite macrostructure in those areas.

Microbialite height and accommodation space

Geomorphological evidence and historical reports facilitate the reconstruction of lake level variations in Laguna de Los Cisnes (Fig. 11A). The presence of thick soils and extensive vegetation below the highest palaeoshoreline at 13 m a.s.l. confirms the older nature of the associated initial lacustrine episode. This highstand

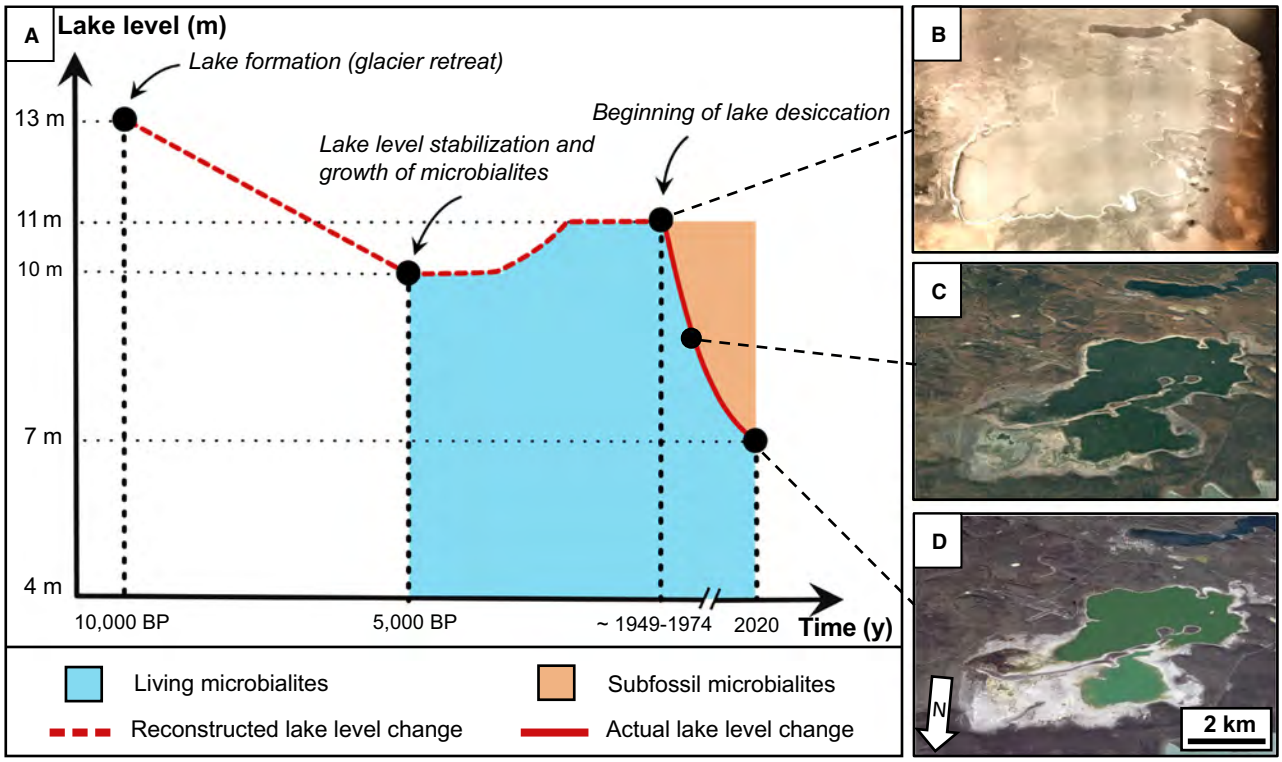

Fig. 11. (A) Lake level variations of Laguna de Los Cisnes reconstructed using palaeoshorelines, microbialites macro-morphologies and historical data. This curve is related to the extent of the active (blue area) and subfossil microbialites (orange area) over time. Between around 5000 BP and 1949 to 1974, the lake level probably fluctuated with an amplitude reaching 1 m maximum, as indicated by compound morphologies of microbialites in the lake. However, the exact amplitude, timing and frequency of these variations are still unclear. Aerial (B), and satellite (C) and (D) images on the right show the progressive lake level fall of anthropic origin during the last century.

was followed by a first lake level regression, likely related to the retreat of the Magellan glacial lobe and associated meltwater at the end of the Last Glacial Maximum. Subsequently, the water level stabilized, forming a smaller lake with a second palaeoshoreline at 11 m a.s.l. (Fig. 11A and B). During this episode, microbialites first appeared in the basin, likely in response to geochemical changes in the lake associated with the first lacustrine regression. The wide bands of dry beaches below the second shoreline (11 m a.s.l.), testify to another, and more recent, lacustrine regression down to today's lake surface (Figs 1, 2A and 11D). The cause of this massive drying is related to the anthropic detour of the main tributary of the lake, the Casa De Lata (Silva Garay *et al.*, 2014). A 1949 aerial photograph reveals no evidence of desiccation (Fig. 11B), yet by 1974, the emergence of dry beaches was noted by Jory *et al.* (1974), marking the onset of the lake regression within this timeframe. The decrease in lake level continues to the present day, although the process has reportedly slowed in recent years (Cordero, 2007). The associated 4 m lake level drop generated a substantial lateral retreat of the submerged area, reaching 3 km in the low gradient north-eastern basin (Figs 2A and 11D). This event radically altered the development of the microbialites in Laguna de Los Cisnes, exposing the buildups that were growing above the current lake level and limiting the microbialites active growth areas to the flooded regions of the basin, now located below 7 m a.s.l.

A link between height zonation and substrate topography

Along a shore to lake coastal transect in Laguna de Los Cisnes (Y–Y′ axis on Fig. 2A), a sequence of microbialite zones with distinct morphologies is observed (Fig. 9A), reflecting a 'zonation of relief' documented in prior research (Borch *et al.*, 1977; Osborne *et al.*, 1982; Cohen & Thouin, 1987; Burne & Moore, 1993; Wattinne *et al.*, 2003; Harris *et al.*, 2013; Bouton *et al.*, 2016; Roche *et al.*, 2018). This

gradient showcases columnar buildups, characteristic of deeper environments, transitioning to dish-shaped microbialites in shallower, nearshore areas (Fig. 9A). Remarkably, the vertical height of algal–microbial buildups in Laguna de Los Cisnes is solely influenced by changes in substrate topography, deepening towards the centre of the basin. Simultaneously, the top of all LLC microbialites is homogeneously located at the same altitude: 11 m a.s.l. This level, also associated with the lateral extension limit of microbialites in the basin, corresponds to the surface of the most recent palaeolake. The rapid disappearance of organo-sedimentary deposits above this surface, once delineating the boundary between submerged and emerged areas of the basin, can be attributed to the incapability of the algal–microbial communities responsible for building the microbialites to survive in the subaerial domain.

These findings indicate that topographic changes along the coastal profile define the available vertical space for microbialite growth, or accommodation space, thereby controlling the morphological gradient of microbialites (height-to-width ratio) perpendicular to the coastline. However, encrusting microbialites diverge from this pattern by not following the typical crater-like architecture and showing limited vertical growth, even where accommodation space is maximal. Despite the scarcity of studies on living microbialites underwater, growth limitation or total disappearance of microbialites beyond a certain depth seems to be a common phenomenon (Cloud, 1942; Eggleston & Dean, 1976; Winsborough *et al.*, 1994), indicating that factors other than accommodation space affect their vertical development in the deepest regions of the basin. Light availability, crucial for the phototrophic organisms (green algae and cyanobacteria) predominant in LLC algal–microbial communities, emerges as a key limiting factor. Presumably, a 4 m higher lake level existing before 1949 would have significantly reduced light penetration and photosynthetic rates in central LLC. Consequently, algal–microbial carbonate growth was likely slowed in these areas, occurring only at the surface of lake bottom irregularities, which likely promoted this process.

Compound microbialites and temporal changes of accommodation space

In parallel to the lateral morphological gradients previously described in Laguna de Los Cisnes, a stacking of distinct microbialite morphotypes (so-called 'compound' microbialites) also develops in a vertical direction (Fig. 9B). Similar macrostructural transitions are widespread in East African Rift lakes, where microbial constructions consist of successive encrustations with specific morphologies (Vincens *et al.*, 1986; Casanova, 1987; Casanova & Hillaire-Marcel, 1992). In most of these deposits, the internal structure exhibits a discontinuous surface separating different generations of encrustation, interpreted as a period of growth interruption. In LLC microbialites, this discontinuity is macrostructural, characterized by different generations of morphologically distinct algal–microbial buildups that develop successively one after the other. Because the height of each microbialite generation is a function of the accommodation space contemporary with its development, the vertical morphological zonation of the microbialites in Laguna de Los Cisnes is likely indicative of successive fluctuations in lake level – and accommodation space – throughout time.

Limitation of environmental influences and role of biological processes

Previous sections have underlined the importance of environmental factors like hydrodynamics and accommodation space in shaping the macrostructural diversity of microbialites in Laguna de Los Cisnes. However, it can also be argued that the role of these abiotic processes is somewhat 'limited' to sculpting the shared fundamental architecture (the crater) for diverse morphological variants. Because the basic crater organization is common to all of the previously described morphotypes occurring under distinct depositional environments (encrusting microbialites excepted), the abiotic processes mentioned above fail to explain this fundamental aspect of microbialite morphogenesis in Laguna de Los Cisnes. The origin of the initial hollow dome remains enigmatic, as does its connection to the various final morphotypes observed in the basin. Crater-shaped microbialites are rarely documented in the literature, and the hypotheses proposed for their genesis (substrate inheritance, preferential growth and erosion, and gas evolution) lack complete validation (Ginsburg, 1955; Logan, 1961; Leventhal & Hosterman, 1982). The 'Ring Bioherms' of the Great Salt Lake (GSL), USA, are well-documented contemporary analogues, and various models have attempted to explain their origin. In protected areas, GSL bioherms develop rounded shapes around partially exposed shoreline reliefs, promoting selective

growth in the more favourable marginal zones that maintain continuous contact with water. Conversely, in high-energy settings, GSL bioherms exhibit elongated morphologies with a raised outer rim because central microbialite growth is inhibited by nearshore erosional processes (Carozzi, 1962; Della Porta, 2015; Baskin *et al.*, 2022).

Lithification of algal–microbial communities in Laguna de Los Cisnes

In Laguna de Los Cisnes, microbialites are closely associated with floating algal–microbial communities dominated by the green alga *Percursaria percursa*. These floating biofilms gradually lithify on microbialite surfaces (Fig. 4B, C and D), initiated by the encrustation of *Percursaria percursa* (Fig. S2). The alga's resemblance to the tubular microstructures in LLC microbialites strongly suggests that these structures likely persist as remnants of algal encrustation following filament decomposition (Figs 6 and S2). These microstructures share morphological similarities with other algal microfossils documented in the microbialites of the Ries crater (Germany; Riding, 1979; Arp, 1995), the calcareous tufa in Mono Lake (USA; Scholl & Taft, 1964) and fluvial tufa worldwide (Zhang *et al.*, 2001; Arenas *et al.*, 2010, 2014; Della Porta, 2015). Observations in Lake Winnipegosis (Canada) also revealed mineral accumulation on *Percursaria percursa* filaments, suggesting its role in limestone tufa formation in the basin (Londry *et al.*, 2005; Grasby & Londry, 2007). Similar to other green algae species involved in algal–microbial bioherm formation, calcification in *Percursaria percursa* may be triggered by the photosynthetic assimilation of CO_2 by the alga itself (Riding, 1979). Epiphytic organisms like cyanobacteria or diatoms present in the mat may also contribute to the passive encrustation of the green alga filaments (Stirn, 1964; Arp, 1995). The arrangement of micritic clots around *Percursaria percursa* microfossils (Fig. 6) underscores that algal mineralization initiates the lithification of the algal–microbial biofilm. The irregular framework of clotted peloidal micrite/microsparite is characteristic of microbial automicrite (Della Porta, 2015), likely resulting from EPS mineralization around *Percursaria percursa* filaments. The mineralization of EPS, likely produced by *Percursaria percursa* and/or associated cyanobacteria, is not yet fully understood but appears linked to biofilm degradation on microbialite surfaces, as found in other studies (Dupraz *et al.*, 2004). The decomposition of shrimp eggs, ubiquitous in the living algal–microbial communities of LLC (Fig. 5F), has been proposed to promote bacterially mediated carbonate precipitation in the bioherms of the GSL (Pedone & Folk, 1996). This lithification process effectively preserves the biofilm's structural characteristics within the microbialite microstructure (Fig. 5C, D, E and F). The stacking of folded carbonate layers forming the internal structure of Laguna de Los Cisnes microbialites likely results from the overlay of successive generations of lithified algal–microbial mats (Fig. 5A and B).

Origin of the microbialite crater

The growth stages of this algal–microbial assemblage offer insights into the genesis of the basic crater morphology common to all morphotypes. In the early stages of mat development, the algal–microbial communities form a benthic mat on the LLC sediments' surface (Fig. 4A and E – stage 1). Bubbles, likely oxygen produced by photosynthetic reactions, become trapped within the dense filamentous network, buoying this cohesive assemblage (Fig. 5D). During intense photosynthetic activity, large patches of algal–microbial mats detach from the lake bottom and float on the water surface (Fig. 4C and E – stage 2). When this happens, the lateral sides of the floating section remain connected to the rest of the benthic mat due to the elastic properties of the biofilm (Fig. 4D). This leads to the vertical projection of localized biofilm areas, forming algal–microbial domes in the water column buoyed by gas bubbles. Rapid mineral precipitation likely further solidifies this ensemble, resulting in a dome-shaped morphology (Fig. 4C, D and E – stage 3). As the carbonate dome is entirely hollow, natural erosion causes the structure's roof to collapse, forming the crater morphologies commonly observed in the LLC (Fig. 4E – stage 4; Fig. 7D).

The previously described biological processes, controlled by the metabolic activity of the algal–microbial communities colonizing the basin, drive the initial building stage of the crater-like organo-sedimentary structures in Laguna de Los Cisnes. The uniformity in microbialite structure and composition across the basin, including their fundamental crater architecture, mesostructure and microstructure, can be attributed to the shared influence of a single algal–microbial community. This consistency persists despite variations in morphotypes collected from different locations within the basin, each exposed to unique environmental conditions. During stage

2 of the microbialite development, when the unconsolidated primary algal–microbial dome is still 'malleable' (Fig. 4E – stage 2), this formation model can be linked with the previously mentioned environmental factors. Under intense hydrodynamic conditions, these floating biofilms are likely to drift in the direction of Langmuir cells and waves, generating the elongated precursors of lenticular microbialites. Similarly, during high lake levels, bubbles will transport floating algal–microbial communities over a greater vertical distance until they reach the lake surface, forming a columnar microbialite. These observations align with previous findings, notably in the bioherms of the Great Salt Lake, showing consistent fabric types despite variations in macrostructure reflecting diverse environmental conditions within the basin (Della Porta, 2015; Baskin *et al.*, 2022).

APPLICATION THROUGH SPACE AND TIME

Degree and orientation of microbialite elongation – a proxy for hydrodynamic processes

The elongation of LLC microbialites results from the interplay of two wind-induced environmental factors: Langmuir cells and waves. As the wind intensity increases from west to east, the resulting hydrodynamic effects in the LLC water column become increasingly stronger along this gradient. The microbialites respond to these changes by gradually becoming more elongated towards the east of the basin. Therefore, the length-to-width ratio (L/W) of microbialites reflects the intensity of the physical environment, where mounds (L/W <3) and lenses (L/W >3) attest to calm and high-energy conditions, respectively. While this relationship is well-documented in marine settings (Logan *et al.*, 1964; Hoffman, 1976; Andres & Reid, 2006), it is the first time that wind-driven elongated microbialites are reported in a lake system. These results call for a re-evaluation of elongated fossil microbialites that have been traditionally interpreted as characteristic of open environments (Young, 1974; Bertrand-Sarfati & Awramik, 1992; Bosak *et al.*, 2013), where fetch length and associated hydrodynamic processes are generally much more intense.

The orientation of the microbialite elongation axis is a more complex parameter to constrain, reflecting the interaction between two distinct hydrodynamic processes. Where Langmuir circulations prevail, algal–microbial structures align with wind directions (zone 4, Fig. 2A and B). Alternatively, in regions where these circulations are less influential, wind-induced waves become the primary control that rules the elongation of the deposits, aligning microbialites perpendicular to the shoreline (zone 2, Fig. 2A and B). These insights provide new considerations for understanding modern elongated microbialites, such as those in Hamelin Pool, where the co-occurrence of 'longitudinal stromatolites' and 'seif stromatolites' mirrors the LLC situation, featuring two types of elongated microbialites controlled by distinct hydrodynamic processes with variable intensity over space (Playford *et al.*, 2013; Suosaari *et al.*, 2019b). Concerning the fossil record, various authors have used elongated microbialites to establish the orientation of ancient coastlines (Hoffman, 1967; Trompette, 1969). The new data from LLC highlights the difficulty of linking the morphogenetic features of elongated microbialites with the environmental parameters, especially in the absence of additional information (for example, current or wind patterns).

Height of microbialites – a proxy for accommodation space

Lake level fluctuations significantly influence the morphology and distribution of microbialites by altering the available accommodation space over time. A decrease in lake level reduces accommodation space, causing the emersion of existing microbial buildups and interrupting microbialite growth. The spatial extent of microbialites in the basin thus reflects the maximum altitude reached by the lake during its history. The LLC microbialite complex, consistently reaching 11 m a.s.l., indicates the former lake level under which microbial buildups developed for thousands of years before recent lake desiccation. Conversely, rising lake levels submerge pre-existing algal–microbial structures, prompting the algal–microbial carbonate factory to colonize newly inundated zones. If this 'highstand' remains stable for long enough, the concomitant increase in accommodation space induces the growth of a new morphotype atop the previous one. Compound microbialites of Laguna de Los Cisnes probably reflect this complex history of lake level variation. A possible interpretation is that after initial stabilization of the lake level at 10 m a.s.l., where the first generation of microbialites (basal morphotype) formed, a second

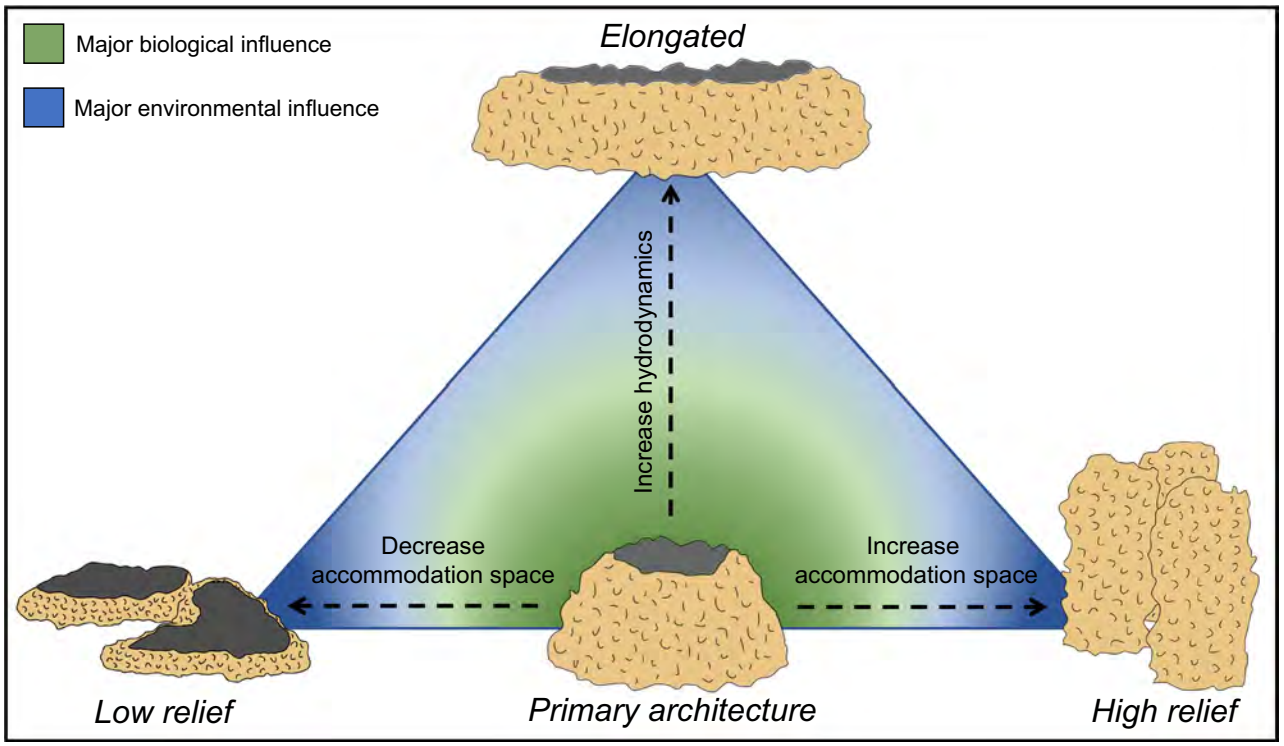

Fig. 12. Model summarizing the relative impact of biological and environmental parameters on the morphogenesis of Laguna de Los Cisnes (LLC) microbialites at the macroscopic scale.

generation (summit morphotype) was superimposed late after a new lacustrine transgression at 11 m a.s.l. (Fig. 11A). Therefore, each generation of microbialites likely represents a specific episode of lake filling, documenting changes in water depth as 'deepening upward' depositional sequences. Furthermore, since microbialites tend to fill the vertical accommodation space under a given lake level, the maximum size of the algal–microbial construction can be used to infer the minimum duration of lake level stabilization. Given the absence of discontinuities in the internal structure of the LLC microbialites and considering the highest growth rate encountered in the literature (1 mm/year; Jahnert & Collins, 2012) the construction of the tallest structures (about 5 m) would have required a stability period of at least 5000 years (Fig. 11A).

Biotic versus abiotic influence

By modifying the morphology of the primary algal dome, hypothesized as a precursor of the basic microbialite crater architecture, abiotic factors rule the macrostructural diversity of organo-sedimentary buildups in the LLC. This relationship establishes columnar microbialites as reliable indicators of palaeoenvironments with sufficient accommodation space, while elongated forms signal the impact of intense hydrodynamic processes (Fig. 12). Therefore, a correct interpretation of the microbialite morphogenesis within the geological record is valuable for reconstructing geological events from a sequential stratigraphy perspective. For example, elongated microbialites overlain by columnar forms may indicate deepening depositional domains with reduced current-related energy. Now, if such interpretation remains correct in high amplitude physical environments, when the intensity of the abiotic parameters decreases, the biotic contribution to the macro-morphogenesis of microbialites becomes dominant (Fig. 12). In such weak physical environments, microbialite macrostructure no longer reflects the environmental forces of the depositional environment but rather the biological processes leading to the building of an initial architectural unit represented by the crater (Fig. 12).

These findings improve previous models that emphasized environmental factors as the primary driver of microbialite macrostructure

(Trompette, 1982; Grotzinger & Knoll, 1999; Dupraz *et al.*, 2004). Analysis of microbialites in Laguna de Los Cisnes suggests that, although abiotic environmental stresses play a significant role in their macroscopic morphogenesis, they are secondary to biological factors. Consequently, the environmental signature on the microbialites macrostructure is only visible in high-energy environments, and thus depends on the depositional setting, while the biological fingerprint is more comprehensive. This model's applicability extends beyond lacustrine systems to marine environments, where abiotic factors are expected to exert a more pronounced influence due to greater hydrodynamic forces and other variables such as tidal currents (Dill *et al.*, 1986), compared to lacustrine settings. These observations also provide critical insight into the interpretation of microbialite morphologies in the geological record. Depending on the system, microbialites may align closer to fossils, where macrostructure reflects the activity of carbonate-building organisms, or to sedimentary structures, where morphology results from interactions with physical (abiotic) factors. Despite significant diversity in microbialite shapes across space and time, a universal model is put forward to interpret their morphology and uncover the dual influence of environmental and biological factors shaping them. The initial step involves identifying the fundamental morphological pattern present in all deposits, which directly indicates the growth mode of the algal–microbial communities. Subsequently, variations in this primary architecture can be analysed to establish further connections with the environmental parameters of the specific depositional environment.

Beyond physical factors, like accommodation space and hydrodynamics, chemical environmental conditions, such as alkalinity and salinity, may indirectly influence microbialite macrostructure by guiding the selection of algal–microbial communities and the timing of their lithification (Della Porta, 2015; Lindsay *et al.*, 2017; Della Porta *et al.*, 2022). This suggests that varying chemical conditions could lead to distinct action–response mechanisms between algal–microbial assemblages and the environment, potentially resulting in microbialites with varied macro-morphologies compared to those observed in Laguna de Los Cisnes. Moreover, the algal–microbial consortia influencing microbialite shapes exhibit significant temporal variability. The emergence of eukaryotic algae, crucial to microbialite formation in Laguna de Los Cisnes, dates back approximately 1.4 billion years (Schopf & Oehler, 1976), representing a period where their role in microbialite construction became increasingly prominent (Monty, 1974). Before this evolutionary juncture, microbialites primarily originated from prokaryotic organisms (Schopf, 1987), which might respond differently to physicochemical factors. Applying the proposed conceptual model to diverse microbialite systems across various spatial and temporal contexts will enhance understanding of the intricate interplay between abiotic factors and diverse algal–microbial communities, elucidating their specific impact on microbialite macrostructure.

CONCLUSIONS

This study investigated the impact of biological and environmental factors on the macroscopic morphogenesis of Laguna de Los Cisnes (LLC) microbialites, revealing five primary morphotypes: mounds, columns, lenses, dish-shaped and crusts. Physical environmental parameters strongly influence microbialite morphology and morphotype distribution across the basin. Microbialite shape results from a delicate balance between hydrodynamic processes and accommodation space, with small relative changes in the intensity of one or the other producing distinct macrostructures. However, this approach does not fully account for some prominent macroscopic features of LLC microbialites. The observed morphotypes essentially represent variations of a primary crater architecture, likely shaped by biological processes. In settings with intense physical parameters, such as strong currents or steep bathymetry, the environmental imprint predominantly influences microbialite morphogenesis. Conversely, in areas with weak physical forces, algal–microbial communities drive macrostructure development. Physical environmental factors exert influence within defined spatial and temporal boundaries, with biological factors prevailing outside these limits. Given the ancient and enduring nature of microbialites, decoding the dual biological and environmental influences recorded in their macrostructure offers crucial insights to unravel the cradle and evolution of life on Earth over the last 3.4 billion years. The modern and subfossil lacustrine microbialites of Laguna de Los Cisnes provide an ideal environment to validate concepts and test hypotheses, enhancing the understanding of this long-debated duality.

ACKNOWLEDGEMENTS

We thank Associate Editor Giovanna Della Porta and two anonymous reviewers for their constructive comments. We also acknowledge Chief Editor Alexander Brasier for guidance through the editorial process. We thank Camille Thomas for guidance in the lab; the inhabitants of the town of Porvenir for their warm welcome; Monica Saleme for her assistance in the field; Andres Bilmes for providing modelling data of Laguna de Los Cisnes; and Davide Carraro for assistance with the X-ray Diffractometer. This work has been supported by an Augustin Lombard grant from the SPHN Society of Geneva. We also acknowledge support from the Swiss National Science Foundation. Project Nr. SNF200020_188571. Open access funding provided by Universite de Geneve.

DATA AVAILABILITY STATEMENT

The data that support the findings of this study are available from the corresponding author upon reasonable request.

REFERENCES

Allen, J.R.L. (1969) Erosional current marks of weakly cohesive mud beds. *J. Sediment. Res.*, **39**, 607–623.

Andres, M.S. and **Reid, R.** (2006) Growth morphologies of modern marine stromatolites: A case study from Highborne Cay, Bahamas. *Sediment. Geol.*, **185**, 319–328.

Arenas, C., **Osácar, C.**, **Sancho, C.**, **Vázquez-Urbez, M.**, **Auqué, L.** and **Pardo, G.** (2010) Seasonal record from recent fluvial tufa deposits (Monasterio de Piedra, NE Spain): sedimentological and stable isotope data. *Geol. Soc. Lond. Spec. Publ.*, **336**, 119–142.

Arenas, C., **Vázquez-Urbez, M.**, **Auqué, L.**, **Sancho, C.**, **Osácar, C.** and **Pardo, G.** (2014) Intrinsic and extrinsic controls of spatial and temporal variations in modern fluvial tufa sedimentation: A thirteen-year record from a semi-arid environment. *Sedimentology*, **61**, 90–132.

Arp, G. (1995) Lacustrine Bioherms, Spring Mounds, and Marginal Carbonates of the Ries-lmpact-Crater (Miocene, Southern Germany). *Facies*, **33**, 35–89.

Auer, V. (1956) The Pleistocene of Fuego-Patagonia: The ice and interglacial ages. *Suomalainen Tiedeakatemia*, **49**, 602–604.

Awramik, S.M. (1992) The history and significance of stromatolites. In: *Early Organic Evolution: Implications for Mineral and Energy Resources* (Eds Schidlowski, M., Golubic, S., Kimberley, M.M., McKirdy, D.M. and Trudinger, P.A.), pp. 435–449. Springer, Berlin, Heidelberg.

Bagnold, R.A. (1953) The surface movement of blown sand in relation to meteorology. *Res. Counc. Isr. Spec. Publ.*, **2**, 89–96.

Baskin, R.L., **Della Porta, G.** and **Wright, V.P.** (2022) Characteristics and controls on the distribution of sublittoral microbial bioherms in Great Salt Lake, Utah: Implications for understanding microbialite development. *Depositional Rec.*, **8**, 39–66.

Basso, D., **Bracchi, V.A.** and **Favalli, A.N.** (2013) Microbialite formation in southern Sinai (Egypt). *Facies*, **59**, 7–18.

Bertrand-Sarfati, J. and **Awramik, S.M.** (1992) Stromatolites of the Mescal Limestone (Apache Group, middle Proterozoic, central Arizona): Taxonomy, biostratigraphy, and paleoenvironments. *Geol. Soc. Am. Bull.*, **104**, 1138–1155.

Bertrand-Sarfati, J. and **Walter, M.R.** (1981) Stromatolite biostratigraphy. *Precambrian Res.*, **15**, 353–371.

Borch, C.C., **Bolton, B.** and **Warren, J.K.** (1977) Environmental setting and microstructure of subfossil lithified stromatolites associated with evaporites, Marion Lake, South Australia. *Sedimentology*, **24**, 693–708.

Bosak, T., **Knoll, A.H.** and **Petroff, A.P.** (2013) The Meaning of Stromatolites. *Annu. Rev. Earth Planet. Sci.*, **41**, 21–44.

Bourillot, R., **Vennin, E.**, **Dupraz, C.**, **Pace, A.**, **Foubert, A.**, **Rouchy, J.-M.**, **Patrier, P.**, **Blanc, P.**, **Bernard, D.**, **Lesseur, J.** and **Visscher, P.T.** (2020) The Record of Environmental and Microbial Signatures in Ancient Microbialites: The Terminal Carbonate Complex from the Neogene Basins of Southeastern Spain. *Minerals*, **10**, 276.

Bouton, A., **Vennin, E.**, **Boulle, J.**, **Pace, A.**, **Bourillot, R.**, **Thomazo, C.**, **Brayard, A.**, **Désaubliaux, G.**, **Goslar, T.**, **Yokoyama, Y.**, **Dupraz, C.** and **Visscher, P.T.** (2016) Linking the distribution of microbial deposits from the Great Salt Lake (Utah, USA) to tectonic and climatic processes. *Biogeosciences*, **13**, 5511–5526.

Burne, R.V. and **Moore, C.** (1993) Microatoll Microbialites of Lake Clifton, Western Australia: Morphological Analogues of Cryptozoön proliferum Hall, the First Formally-named Stromatolite. *Facies*, **29**, 149–168.

Button, A. and **Vos, R.G.** (1977) Subtidal and intertidal clastic and carbonate sedimentation in a macrotidal environment: an example from the lower proterozoic of South Africa. *Sediment. Geol.*, **18**, 175–200.

Carozzi, A.V. (1962) Observations on Algal Biostromes in the Great Salt Lake, Utah. *J. Geol.*, **70**, 246–252.

Casanova, J. (1987) Stromatolites et hauts niveaux lacustres pléistocènes du bassin Natron-Magadi (Tanzanie-Kenya). *Sci. Géologiques Bull.*, **40**, 135–153.

Casanova, J. and **Hillaire-Marcel, C.** (1992) Chronology and paleohydrology of late Quaternary high lake levels in the Manyara basin (Tanzania) from isotopic data (^{18}O, ^{13}C, ^{14}C, Th/U) on fossil stromatolites. *Quatern. Res.*, **38**, 205–226.

Chubarenko, I., **Esiukova, E.**, **Bagaev, A.**, **Isachenko, I.**, **Demchenko, N.**, **Zobkov, M.**, **Efimova, I.**, **Bagaeva, M.** and **Khatmullina, L.** (2018) Behavior of microplastics in coastal zones. In: *Microplastic Contamination in Aquatic Environments* (Ed. Zeng, E.Y.), pp. 175–223. Elsevier, Amsterdam.

Cloud, P.E. (1942) Notes on stromatolites. *Am. J. Sci.*, **240**, 363–379.

Cohen, A.S. and **Thouin, C.** (1987) Nearshore carbonate deposits in Lake Tanganyika. *Geology*, **15**, 414–418.

Cordero, H. (2007) El Lago de los Cisnes, sitio de concentración de las aves en Tierra del Fuego. *La Chiricoca*, **4**, 6–10.

Coronato, A., **Salemme, M.** and **Rabassa, J.** (1999) Palaeoenvironmental conditions during the early peopling of southernmost South America (Late Glacial-Early Holocene, 14-8 ka BP). *Quat. Int.*, **53**, 77–92.

Coulson, K.P. (2016) Microbialite elongation by means of coalescence: an example from the middle Furongian (upper Cambrian) Notch Peak Formation of western Utah. *Facies*, **62**, 20.

Della Porta, G. (2015) Carbonate build-ups in lacustrine, hydrothermal and fluvial settings: comparing depositional geometry, fabric types and geochemical signature. *Geol. Soc. Lond. Spec. Publ.*, **418**, 17–68.

Della Porta, G., **Hoppert, M.**, **Hallmann, C.**, **Schneider, D.** and **Reitner, J.** (2022) The influence of microbial mats on travertine precipitation in active hydrothermal systems (Central Italy). *Depositional Rec.*, **8**, 165–209.

Des Marais, D.J. (1991) Microbial mats, stromatolites and the rise of oxygen in the Precambrian atmosphere. *Glob. Planet. Change*, **97**, 93–96.

Dethleff, D. and **Kempema, E.W.** (2007) Langmuir circulation driving sediment entrainment into newly formed ice: Tank experiment results with application to nature (Lake Hattie, United States; Kara Sea, Siberia). *J. Geophys. Res. Oceans*, **112**, 3259.

Diáz Balocchi, L., **Cao, S.J.** and **Bedoya Agudelo, E.L.** (2021) An introduction to the geology of Tierra del Fuego. In: *Geological Resources of Tierra del Fuego* (Ed. Acevedo, R.D.), pp. 1−17. Springer International Publishing, Cham.

Dierssen, H.M., **Zimmerman, R.C.** and **Burdige, D.J.** (2009) Optics and remote sensing of Bahamian carbonate sediment whitings and potential relationship to wind-driven Langmuir circulation. *Biogeosciences*, **6**, 487–500.

Dill, R.F., **Shinn, E.A.**, **Jones, A.T.**, **Kelly, K.** and **Steinen, R.P.** (1986) Giant subtidal stromatolites forming in normal salinity waters. *Nature*, **324**, 55–58.

Dupraz, C., **Visscher, P.T.**, **Baumgartner, L.K.** and **Reid, R.P.** (2004) Microbe–mineral interactions: early carbonate precipitation in a hypersaline lake (Eleuthera Island, Bahamas). *Sedimentology*, **51**, 745–765.

Dzulynski, S. and **Walton, E.K.** (1965) *Sedimentary Features of Flysch and Greywackes*. Elsevier Pub. Co., Amsterdam.

Eggleston, J.R. and **Dean, W.E.** (1976) Freshwater stromatolitic bioherms in Green Lake, New York. In: *Developments in Sedimentology* (Ed. Walter, M.R.), Vol. **20**, pp. 479–488. Elsevier, Amsterdam.

Feldmann, M. and **McKenzie, J.A.** (1998) Stromatolite-thrombolite associations in a modern environment, Lee Stocking Island, Bahamas. *PALAIOS*, **13**, 201–212.

Fuentes, N. and **Gajardo, G.** (2017) A glimpse to Laguna de los Cisnes, a field laboratory and natural monument in the Chilean Patagonia. *Lat. Am. J. Aquat. Res.*, **45**, 491–495.

Gargett, A., **Wells, J.**, **Tejada-Martinez, A.E.** and **Grosch, C.E.** (2004) Langmuir supercells: A mechanism for sediment resuspension and transport in shallow seas. *Science*, **306**, 1925–1928.

Gebelein, C.D. (1976) Open marine subtidal and intertidal stromatolites (Florida, The Bahamas and Bermuda). In: *Developments in Sedimentology* (Ed. Walter, M.R.), Vol. **20**, pp. 381–388. Elsevier, Amsterdam.

Ginsburg, R.N. (1955) Recent stromatolitic sediments from south Florida. *J. Sediment. Res.*, **25**, 129.

Ginsburg, R.N. (1991) Controversies about stromatolties: vices and virtues. In: *Controversies in Modern Geology; Evolution of Geological Theories in Sedimentology, Earth History and Tectonics* (Eds Müller, D.W., McKenzie, J.A. and Weissert, H.), pp. 25–36. Academic Press, London.

Ginsburg, R.N. and **Planavsky, N.J.** (2008) Diversity of Bahamian Microbialite Substrates. In: *Links between Geological Processes, Microbial Activities & Evolution of Life: Microbes and Geology* (Eds Dilek, Y., Furnes, H. and Muehlenbachs, K.), pp. 177–195. Springer, Dordrecht.

Glennie, K.W. (1970) *Desert Sedimentary Environments*, p. 222. Elsevier Pub. Co, Amsterdam; New York, NY.

Grasby, S.E. and **Londry, K.L.** (2007) Biogeochemistry of hypersaline springs supporting a mid-continent marine ecosystem: An analogue for martian springs? *Astrobiology*, **7**, 662–683.

Grey, K. and **Awramik, S.** (2020) Handbook for the study and description of microbialites. *Geol. Surv. West. Aust.*, **147**, 278.

Grotzinger, J.P. and **Knoll, A.H.** (1999) Stromatolites in precambrian carbonates: evolutionary mileposts or environmental dipsticks? *Annu. Rev. Earth Planet. Sci.*, **27**, 313–358.

Grotzinger, J.P. and **Rothman, D.H.** (1996) An abiotic model for stromatolite morphogenesis. *Nature*, **383**, 423–425.

Harris, P.M., **Ellis, J.** and **Purkis, S.J.** (2013) Assessing the extent of carbonate deposition in early rift settings. *AAPG Bull.*, **97**, 27–60.

Hoffman, P. (1967) Algal stromatolites: Use in stratigraphic correlation and paleocurrent determination. *Science*, **157**, 1043–1045.

Hoffman, P. (1976) Stromatolite morphogenesis in Shark Bay, Western Australia. In: *Developments in Sedimentology* (Ed. Walter, M.R.), Vol. **20**, pp. 261–271. Elsevier, Amsterdam.

Jahnert, R.J. and **Collins, L.B.** (2012) Characteristics, distribution and morphogenesis of subtidal microbial systems in Shark Bay, Australia. *Mar. Geol.*, **303–306**, 115–136.

Jory, J.E., **Venegas, C.**, **C.** and **Texera, W.A.** (1974) La avifauna del parque Nacional "Laguna de Los Cisnes" Tierra del Fuego, Chile. *Anales del Instituto de la Patagonia*, **5**, 131–154.

Kennard, J.M. and **Burne, R.V.** (1989) Stromatolite newsletter. *Bur. Min. Res., Geol. Geophys.*, **14**, 42.

Krylov, I.N. (1976) Approaches to the classification of stromatolites. *Develop. Sedimentol.*, **20**, 31–43.

Langmuir, I. (1938) Surface motion of water induced by wind. *Science*, **87**, 119–123.

Leibovich, S. (2009) Langmuir circulation and instability. In: *Elements of Physical Oceanography: A derivative of the Encyclopedia of Ocean Sciences* (Eds Steele, J.H., Thorpe, S.A. and Turekian, K.K.), Vol. **124**, pp. 288−297. Elsevier, Amsterdam.

Leventhal, J.S. and **Hosterman, J.W.** (1982) Chemical and mineralogical analysis of devonian black-shale samples from Martin County, Kentucky; Carroll and Washington counties, Ohio; Wise County, Virginia; and Overton County, Tennessee, U.S.A. *Chem. Geol.*, **37**, 239–264.

Lindsay, M.R., **Anderson, C.**, **Fox, N.**, **Scofield, G.**, **Allen, J.**, **Anderson, E.**, **Bueter, L.**, **Poudel, S.**, **Sutherland, K.**, **Munson-McGee, J.H.**, **Van Nostrand, J.D.**, **Zhou, J.**, **Spear, J.R.**, **Baxter, B.K.**, **Lageson, D.R.** and **Boyd, E.S.** (2017) Microbialite response to an anthropogenic salinity

gradient in Great Salt Lake, Utah. *Geobiology*, **15**, 131–145.

Logan, B.W. (1961) Cryptozoon and Associate Stromatolites from the Recent, Shark Bay, Western Australia. *J. Geol.*, **69**, 517–533.

Logan, B.W., **Rezak, R.** and **Ginsburg, R.N.** (1964) Classification and Environmental Significance of Algal Stromatolites. *J. Geol.*, **72**, 68–83.

Logan, B.W., **Hoffman, P.** and **Gebelein, C.D.** (1974) Algal Mats, Cryptalgal Fabrics, and Structures, Hamelin Pool, Western Australia. *AAPG Bull.*, **41**, 140–194.

Londry, K.L., **Badiou, P.H.** and **Grasby, S.E.** (2005) Identification of a marine green Alga *Percursaria percursa* from hypersaline springs in the middle of the North American Continent. *Can. Field-Nat.*, **119**, 82.

Mariotti, G., **Perron, J.T.** and **Bosak, T.** (2014) Feedbacks between flow, sediment motion and microbial growth on sand bars initiate and shape elongated stromatolite mounds. *Earth Planet. Sci. Lett.*, **397**, 93–100.

McCulloch, R.D., **Clapperton, C.M.**, **Rabassa, J.** and **Currant, A.P.** (1997) The natural setting. The glacial and post-glacial environmental history of Fuego-Patagonia. In: *Patagonia: natural history, prehistory and ethnography at the uttermost end of the Earth* (Eds McEwan, C., Borrero, L. and Prietto, A.), pp. 12−31. Princeton University Press, Princeton.

McNamara, K.J. and **Awramik, S.M.** (1992) Stromatolites: a key to understanding the early evolution of life. *Sci. Prog.*, **1933**, 345–364.

Monty, C. (1974) Precambrian background and Phanerozoic history of stromatolitic communities, an overview. *Annales de la Société Géologique de Belgique*, **96**, 585–624.

Osborne, R.H., **Licari, G.R.** and **Link, M.H.** (1982) Modern lacustrine stromatolites, Walker Lake, Nevada. *Sediment. Geol.*, **32**, 39–61.

Pedone, V.A. and **Folk, R.L.** (1996) Formation of aragonite cement by nannobacteria in the Great Salt Lake, Utah. *Geology*, **24**, 763–765.

Peel, M.C., **Finlayson, B.L.** and **Mcmahon, T.A.** (2007) Updated world map of the Köppen-Geiger climate classification. *Hydrol. Earth Syst. Sci.*, **11**, 1633–1644.

Planavsky, N.J. and **Ginsburg, R.N.** (2009) Taphonomy of modern marine bahamian microbialites. *PALAIOS*, **24**, 5–17.

Playford, P.E. (1980) Environmental controls on the morphology of modern stromatolites at Hamelin Pool, Western Australia. *West. Aust. Geol. Surv. Annu. Rep.*, **1979**, 73–77.

Playford, P.E., **Cockbain, A.E.**, **Berry, P.F.**, **Roberts, A.P.**, **Haines, P.W.** and **Brooke, B.P.** (2013) *The Geology of Shark Bay*, p. 281. Geological Survey of Western Australia, Perth.

Rabassa, J. and **Clapperton, C.M.** (1990) Quaternary glaciations of the southern Andes. *Quat. Sci. Rev.*, **9**, 153–174.

Rabassa, J., **Coronato, A.**, **Bujalesky, G.**, **Salemme, M.**, **Roig, C.**, **Meglioli, A.**, **Heusser, C.**, **Gordillo, S.**, **Roig, F.**, **Borromei, A.** and **Quattrocchio, M.** (2000) Quaternary of Tierra del Fuego, Southernmost South America: an updated review. *Quat. Int.*, **68–71**, 217–240.

Riding, R. (1979) Origin and diagenesis of lacustrine algal bioherms at the margin of the Ries crater, Upper Miocene, southern Germany. *Sedimentology*, **26**, 645–680.

Roche, A., **Vennin, E.**, **Bouton, A.**, **Olivier, N.**, **Wattinne, A.**, **Bundeleva, I.**, **Deconinck, J.-F.**, **Virgone, A.**, **Gaucher, E.C.** and **Visscher, P.T.** (2018) Oligo-Miocene lacustrine microbial and metazoan buildups from the Limagne Basin (French Massif Central). *Palaeogeogr. Palaeoclimatol. Palaeoecol.*, **504**, 34–59.

Scholl, D.W. and **Taft, W.H.** (1964) Algae, contributors to the formation of calcareous tufa, Mono Lake, California. *J. Sediment. Res.*, **34**, 309–319.

Schopf, J.W. (1987) Precambrian Prokaryotes and Stromatolites. *Ser. Geol. Notes Short Course*, **18**, 20–33.

Schopf, J.W. and **Oehler, D.Z.** (1976) How old are the eukaryotes? *Science*, **193**, 47–49.

Schopf, J.W., **Kudryavtsev, A.B.**, **Czaja, A.D.** and **Tripathi, A.B.** (2007) Evidence of Archean life: Stromatolites and microfossils. *Precambrian Res.*, **158**, 141–155.

Semikhatov, M.A. and **Raaben, M.E.** (2000) Proterozoic stromatolite taxonomy and biostratigraphy. In: *Microbial Sediments* (Eds Riding, R.E. and Awramik, S.M.), pp. 295–306. Springer, Berlin, Heidelberg.

Semikhatov, M.A., **Gebelein, C.D.**, **Cloud, P.**, **Awramik, S.M.** and **Benmore, W.C.** (1979) Stromatolite morphogenesis—progress and problems. *Can. J. Earth Sci.*, **16**, 992–1015.

Serebryakov, S.N. and **Semikhatov, M.A.** (1974) Riphean and recent stromatolites: a comparison. *Am. J. Sci.*, **274**, 556–574.

Silva Garay, A., **Ruiz Bustamante, M.**, **Ivanovich, J.**, **Vergara Recabal, K.**, **Ramírez Mérida, I.**, **Hernandez Bonacich, C.** and **Cano Gallegos, V.** (2014) *Plan de Manejo – Monumento Natural Laguna de Los Cisnes*. Corporación Nacional Forestal, Santiago.

Smith, J.A. (2001) Observations and theories of langmuir circulation: A story of mixing. In: *Fluid Mechanics and the Environment: Dynamical Approaches* (Ed. Lumley, J.L.), pp. 295–314. Springer, Berlin, Heidelberg.

Stirn, A. (1964) *Kalktuffvorkommen und Kalktufftypen der Schwäbischen Alb*. PhD Thesis. Verband d. Dt. Höhlen- und Karstforscher, Munich.

Suosaari, E.P., **Reid, R.P.** and **Andres, M.S.** (2019a) Stromatolites, so what A tribute to Robert N. Ginsburg. *Depositional Rec.*, **5**, 486–497.

Suosaari, E.P., **Reid, R.P.**, **Oehlert, A.M.**, **Playford, P.E.**, **Steffensen, C.K.**, **Andres, M.S.**, **Suosaari, G.V.**, **Milano, G.R.** and **Eberli, G.P.** (2019b) Stromatolite provinces of Hamelin Pool: Physiographic controls on stromatolites and associated lithofacies. *J. Sediment. Res.*, **89**, 207–226.

Talley, L.D., **Pickard, G.L.**, **Emery, W.J.** and **Swift, J.H.** (2011) Dynamical processes for descriptive ocean circulation. In: *Descriptive Physical Oceanography* (Eds Talley, L.D., Pickard, G.L., Emery, W.J. and Swift, J.H.), pp. 1–72. Elsevier, Amsterdam.

Thorpe, S.A. (2004) Langmuir circulation. *Annu. Rev. Fluid Mech.*, **36**, 55–79.

Trompette, R. (1969) Les stromatolites du "precambrien superieur" de l'adrar de Mauritanie (sahara occidental). *Sedimentology*, **13**, 123–154.

Trompette, R. (1982) Upper Proterozoic (1800-570 Ma) stratigraphy: A survey of lithostratigraphic, paleontological, radiochronological and magnetic correlations. *Precambrian Res.*, **18**, 27–52.

Vincens, A., **Casanova, J.** and **Tiercelin, J.J.** (1986) Palaeolimnology of Lake Bogoria (Kenya) during the 4500 BP high lacustrine phase. *Geol. Soc. Lond. Spec. Publ.*, **25**, 323–330.

Walter, M.R. (1972) Stromatolites and the biostratigraphy of the Australian Precambrian and Cambrian. *Spec. Pap. Paleontol.*, **11**, 1–190.

Walter, M.R. (1977) Interpreting Stromatolites: These fossils can tell us much about past organisms and environments

if we can learn to decode their message. *Am. Sci.*, **65**, 563–571.

Wattinne, A., **Vennin, E.** and **De Wever, P.** (2003) Evolution of carbonated, lacustrine environment, with stromatolites: a paleoecological approach (quarry of Montaigu-le-Blin, Limagne graben, Allier, France). *Bull. Société Géologique Fr.*, **174**, 243–260.

Wilson, I.G. (1972) Aeolian Bedforms - Their development and origins. *Sedimentology*, **19**, 173–210.

Winsborough, B.M., **Seeler, J.-S.**, **Golubic, S.**, **Folk, R.L.** and **Maguire, B.** (1994) Recent fresh-water lacustrine stromatolites, stromatolitic mats and oncoids from northeastern Mexico. In: *Phanerozoic Stromatolites II* (Eds Bertrand-Sarfati, J. and Monty, C.), pp. 71–100. Springer, Dordrecht.

Young, G.M. (1974) Stratigraphy, paleocurrents and stromatolites of Hadrynian (Upper Precambrian) rocks of Victoria Island, Arctic Archipelago, Canada. *Precambrian Res.*, **1**, 13–41.

Young, G.M. and **Jefferson, C.W.** (1975) Late Precambrian Shallow Water Deposits, Banks and Victoria Islands, Arctic Archipelago. *Can. J. Earth Sci.*, **12**, 1734–1748.

Young, G.M. and **Long, D.G.F.** (1976) Stromatolites and basin analysis: an example from the upper proterozoic of northwestern Canada. *Palaeogeogr. Palaeoclimatol. Palaeoecol.*, **19**, 303–318.

Zhang, D.D., **Zhang, Y.**, **Zhu, A.** and **Cheng, X.** (2001) Physical mechanisms of river waterfall tufa (travertine) formation. *J. Sediment. Res.*, **71**, 205–216.

Manuscript received 1 August 2023; revision accepted 23 February 2024

Supporting Information

Additional information may be found in the online version of this article:

Appendix S1. The green alga *Percursaria percursa*.

Appendix S2. Mineralogical description of Laguna de Los Cisnes microbialites.

Fig. S1. Satellite image showing the location of the two primary ancient shorelines on the east side of the Laguna de Los Cisnes basin.

Fig. S2. Natural light (A) and polarized light (B) images of the floating algal-microbial community in Laguna de Los Cisnes, highlighting the dominant presence of the green alga *Percursaria percursa*.

Fig. S3. Powder X-ray diffractogram of the layer just beneath the outer surface of the Laguna de Los Cisnes microbialites (M: monohydrocalcite).